EFFECT OF ROUGHNESS ON FLOW MEASUREMENTS IN SLOPING RECTANGULAR CHANNELS WITH FREE OVERFALL

A THESIS SUBMITTED TO

THE GRADUATE SCHOOL OF NATURAL AND APPLIED SCIENCES

OF

THE MIDDLE EAST TECHNICAL UNIVERSITY

BY

CAN ERSEN FIRAT

IN PARTIAL FULFILLMENT OF THE REQUIREMENTS FOR THE DEGREE OF MASTER OF SCIENCE

IN

THE DEPARTMENT OF CIVIL ENGINEERING

FEBRUARY 2004

Approval of the Graduate School of Natural and Applied Sciences

Prof. Dr. Canan ÖZGEN
Director

I certify that this thesis satisfies all the requirements as a thesis for the degree of Master of Science.

Prof. Dr. Erdal ÇOKÇA
Head of Department

This is to certify that we have read this thesis and that in our opinion it is fully adequate, in scope and quality, as a thesis for the degree of Master of Science.

Dr. Şahnaz TİĞREK
Supervisor

Examining Committee Members

Prof. Dr. Melih YANMAZ

Prof. Dr. Metin GER

Assoc. Prof. Dr. İsmail AYDIN

Dr. Şahnaz TİĞREK

Dr. Hande AKÇAKOCA

ABSTRACT

EFFECT OF ROUGHNESS ON FLOW MEASUREMENTS IN SLOPING RECTANGULAR CHANNELS WITH FREE OVERFALL

FIRAT, Can Ersen

M.Sc., Department of Civil Engineering

Supervisor: Dr. Şahnaz TİĞREK

February 2004, 68 pages

The characteristics of the subcritical, critical and supercritical flows at the rectangular free overfall were studied experimentally to obtain a relation between the brink depth and the flow rate. A series of experiments were conducted in a tilting flume with wide range of flow rate and two bed roughness in order to find the relationship between the brink depth, normal depth, channel bed slope and bed roughnesses. An equation was proposed to calculate the flow rate if only the brink depth, roughness, and channel bed slope are known. An alternate iterative solution was offered to calculate discharges if the brink depth and uniform flow depth are known.

Key Words: Brink Depth, End Depth, Free Overfall, Discharge Measurement, Roughness

ÖZ

SERBEST DÜŞÜLÜ EĞİMLİ DİKDÖRTGEN KESİTLİ KANALLARDA YÜZEY PÜRÜZLÜLÜĞÜN AKIM ÖLÇÜMLERİNE ETKİSİ

FIRAT, Can Ersen

Yüksek Lisans, İnşaat Mühendisliği Bölümü

Tez Yöneticisi: Dr. Şahnaz TİĞREK

Şubat 2004, 68 sayfa

Nehir rejimi, kritik rejim ve sel rejiminin dikdörtgen kesitli kanallardaki serbest düşülerdeki davranış biçimi, düşü akım derinliği ve debi arasındaki ilişkiyi elde edebilmek için deneysel olarak incelenmiştir. Düşü akım derinliği, üniform akım derinliği, kanal taban eğimi ve yatak pürüzlülüğü arasındaki ilişkileri tayin edebilmek için geniş bir veri gamında değişen eğimler ve iki farklı taban pürüzlülük değeri için veriler toplanmıştır. Düşü akım derinliği, kanal taban eğimi ve pürüzlülük bilgileri kullanılarak kanal debisinin bulunabileceği bir eşitlik önerilmiştir. Ayrıca sadace düşü akım derinliği ve üniform akım derinliğinden deneme yanılma yoluyla akımın hesaplanabileceği bir alternatif çözüm de önerilmiştir.

Anahtar Kelimeler: Düşü Akım Derinliği, Serbest Düşü, Debi Ölçümü, Pürüzlüklük

To my nephew, Yağız,

ACKNOWLEDGMENTS

In acknowledging the help I received during this study, I would like first of all to express my deepest gratitude and appreciation to Prof. Dr. Metin GER for his precious advice and comment throughout the whole study.

I am thankful to Dr. Şahnaz TİĞREK for her supervision and supportive suggestions throughout this study.

I wish to express my sincere appreciation to Yavuz ÖZEREN for his kind assist and support during the hardest times of my study.

I am grateful to my parents for support and encouraging me with endless patience and love throughout this period. I am indebted to my brother for his motivating support during this study. My special thanks go to İdil S. SOYSEÇKİN, H. Uğraş ÖZTÜRK, Sinem DEMİREL and Çağdaş DEMİRCİOĞLU for their help and support through these hard times.

I am extending my thanks to Laboratory Technicians for their help through my experimental performance.

TABLE OF CONTENTS

LIST OF TABLES

Table

LIST OF FIGURES

Figure

LIST OF SYMBOLS

A	flow area
C_c	contraction coefficient
C_d	weir coefficient
F_0	upstream Froude number
H	summation of velocity and elevation head
H_w	head on the triangular weir
L	length dimension
P	wetted perimeter
Q	discharge
R	hydraulic radius
Re	Reynold's number
S	slope of the energy grade line
S_c	critical bed slope
S_0	bed slope
T	time dimension
V	flow velocity
b	channel width
g	acceleration due to gravity
n	Manning's roughness coefficient
q	discharge per unit width
r^2	root mean square
x_i	i=1,2,3 the optimum horizontal distance from the brink section where normal depth occurs
y_c	critical depth

y_e	brink depth
y_0	upstream normal depth
μ	viscosity
ρ	density
V_0	uniform flow velocity
z	vertical coordinate measured from a reference level
$y_{c,theoretical}$	theoretical critical depth
$q_{theoretical}$	theoretical discharge per unit width
q_{true}	experimental discharge per unit width
P_k	pressure at section k=A,B

CHAPTER 1

INTRODUCTION AND REVIEW OF LITERATURE

1.1 General Information on Free Overall

The overfall refers to the downstream portion of a rectangular channel, horizontal or sloping, terminating abruptly at its lower end. If it is not submerged by the tail water, it is referred to as the free overfall. A vertical drop of a free overfall is a common feature in both natural and artificial channels. Natural drops are formed by river erosion while drop structures are built in irrigation and drainage channels as energy reducing devices especially where the flow is supercritical.

The free overfall is of distinct importance in hydraulic engineering, aside from its close relation to the broad crested weir, for it forms the starting point in computations of the surface curve in non-uniform channel flow in which the discharge spills into an open reservoir at the downstream end.

The study of a free overfall is also important because of possible usage of it as a discharge-measuring device. The problem of the free overfall as a discharge measuring device has attracted considerable interest for almost 70 years and the end depth discharge relationship has been extensively studied by carrying out the

theoretical and experimental studies at free overfall of a channel in order to establish a relationship between the critical depth, y_c and the brink depth (end depth), y_e. Rouse (1936) was the first to point out the possibility of using the free overfall as a flow meter, which needs no calibration. Although the streamlines at the overfall is not parallel, the crest section is that of true minimum energy and hence is the actual section.

1.2 Review of Literature

Rouse (1936) conducted experiments in a horizontal channel and concluded that the brink depth is a constant percentage of the computed critical depth of the parallel flow. He informed that end depth ratio, y_e/y_c =0.715 when Froude number is equal to one. He also calculated the ratio of brink depth and upstream flow depths, for variable upstream Froude number, F_0. He also gave experimentally, non-dimensional plots of flow geometry for the range of $1 \leq F_0 \leq 20$. After Rouse, the researchers were concentrated on the value of end depth ratio, Rajaratham and Muralidhar (1967) reported the value as 0.715 and Krajenhoff and Dommerholt (1977) gave it as 0.714. However some other researchers gave higher values; Gupta et al (1992) reported a value of 0.745, Ferro (1992) reported it to be 0.760 and Bauer and Graf (1971) gave a higher value of 0.781.

On the other hand among several theoretical studies only Ferro (1999) obtained a value of 0.715 . Ali and Sykes (1972) calculated the value as 0.667 by momentum equation and 0.673 by free vortex theory. Hager (1983) and Marchi (1993) reported 0.696 and 0. 706, respectively.

As it can be seen that there are several studies for critical flow on horizontal bed. However this is not a common condition in the field. Beside that it is very difficult to measure flow depth at the critical flow condition.

On the other hand in case of sloping rectangular channels there are limited studies. Rajaratnam and Muralidhar (1964a and 1964b) experimentally investigated the effect of different shapes of the channel cross section. They found that for a subcritical flow, the end depth ratio is nearly constant, whereas for a supercritical flow the end depth ratio rapidly decreases with increasing S_o/S_c values (in Rajaratnam and Muralidhar, 1967). Later Kraijenhoff and Dommerholt (1977) investigated the end depth and the critical depth in a wide rectangular channel with variable slope and roughness. Their y_e/y_c value of 0.714 was not significantly affected by either the mild slopes up to 0.0025 or by the bottom roughness.

These few studies are usually limited to subcritical flow conditions. This is due to the difficulties faced with performing the experiments with a supercritical flow. It is known that when the supercritical flow is concerned every single disturbance creates cross-waves leading to the difficulties in determining the depth of flow and turbulence takes place everywhere, which makes the measurements difficult. On the other hand, in engineering practice we usually face with supercritical flows in sloping channels. Therefore, it becomes necessary to study such flows to have a better design of such hydraulic structures.

Alastair et al. (1998) performed an experimental study of the free overfall in a rectangular channel with differing slopes and bed roughness. The relationship between the upstream critical depth and brink depth was explored and found to be influenced by both the slope and the channel bed roughness, with roughness having a greater effect at steeper slopes. Two empirical equations were proposed for calculating this relationship; the first equation requiring only the channel slope to be known and the second equation requiring knowledge of channel slope and Manning roughness coefficient, n. The accuracy of two equations when used in a method for flow measurements was compared. The first relationship, in which the effects of slope and roughness are aggregated, provided a useful estimate of channel discharge if only the channel slope is known. If both bed roughness and slope are known then

the second relationship could be used to calculate the channel discharge with greater accuracy.

Turan (2002) conducted several experiments in a sloping rectangular channel having smooth bed. The equation given by Alastair was reexamined by those additional data. He concluded that further experiments were needed in order to see the effect of bed roughness.

1.3 Scope of the Study

In the present study the effect of roughness on the brink depth is investigated on both mild and steep slopes. Special attention is given to supercritical flow condition.

The results obtained are presented in the form that would be useful to an engineer designing a hydraulic structure, which includes drops with both subcritical and supercritical flow.

In the thesis Chapter 2 is reserved for theoretical work. Experimental setup and data collecting procedure are given in Chapter 3. In Chapter 4 results and discussions are presented. Finally conclusions and recommendations for further studies are given in Chapter 5.

CHAPTER 2

THEORETICAL CONSIDERATION ON FREE OVERFALL

2.1 General Characteristics of Free Overfall

In the situation of the free overfall, shown in Figure 2.1, flow takes place over a sharp drop. Section B is the location of the brink where mean pressure is less than hydrostatic pressure due to acceleration of the flow. It should also be clear that quite a short distance back from the brink, the vertical accelerations will be small and the pressure will be hydrostatic (Section A). Section A is the location where the flow characteristics are not affected from the brink and the flow is assumed to be uniform. The flow between A and B is not uniform and there is no downstream channel effect on the flow in the case of zero submergence.

In Figure 2.1:

y_0: uniform flow depth

y_c: critical depth

y_e: brink depth

n: the Manning's Roughness Coefficient

P_A: pressure at Section A

P_B: pressure at Section B

q: discharge per unit width

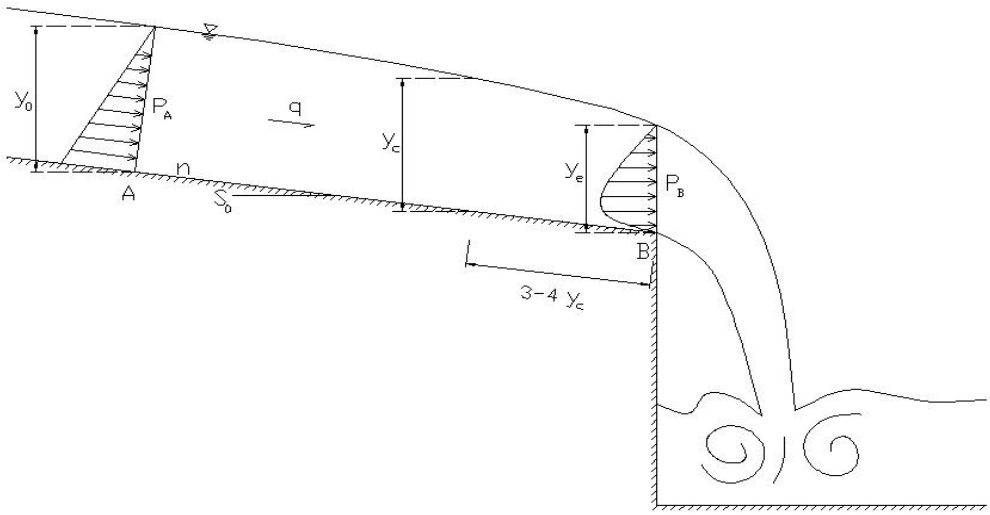

Figure 2.1 The Free Overfall

If the slope of the upstream channel is steep, the flow at A will be supercritical and determined by the upstream conditions. If, on the other hand, the channel slope is mild, horizontal, or adverse the flow at A will be uniform flow.

The local effects of the brink are confined to the region A-B; experiments show this section to be quite short, of order 3-4 times the critical depth in case of mild slopes. Upstream of A the profile will be one of the normal types determined by channel slope and roughness.

Attempts to solve flow analytically usually faced with the difficulty of the modeling the pressure over the brink. Delleur et al. (1956) solved momentum equation by assuming the pressure over the brink is a function of hydrostatic pressure. However a general form of the pressure coefficient have not been proposed yet.

Hager (1983) treated the free overfall by using the extended energy and momentum equations by taking into account of the streamline inclination and curvature. The end depth ratio was estimated by momentum considerations at the brink and upstream sections. Distinction was made between pressure head and flow depth, which coincide only for parallel, horizontal streamlines. His investigation dealt with plane overfalls under the condition of pseudo-uniform flow state. The computations were divided into upstream and downstream zones. The solution found is appropriate for, $F_0 \geq 1$.

There are several studies in which the free fall solved numerically. The potential flow method is used by Montes (1992) and Özsaraç (2002). However in this kind of models the effect of roughness cannot be incorporated with the flow equations.

2.2 End Relationship for Rectangular Cross-section

According to Ferro (1999), the free overfall in a rectangular channel can be assumed to be similar to the flow over a sharp-crested weir of the same section with a weir crest height equal to zero and head above the crest weir is the normal depth.

The flow velocity at the brink section is calculated by applying the Bernoulli equation at any streamlines between section A and the brink section B in Figure 2.1. In accordance with the theoretical procedure applied to compute the discharge over a sharp crested weir, a zero pressure distribution and parallel streamlines at the brink are initially assumed. The discharge, Q, is computed by the following equation:

$$Q = \int_0^{y_0} C_c b\sqrt{2g(H - z)}\, dz = \frac{2b\sqrt{2g}}{3} C_c \left[H^{3/2} - (H - y_0)^{3/2}\right] \qquad (2\text{-}1)$$

where,

V_0: uniform flow velocity

H: $y_0 + V_0^2/2g$ denotes the energy at section A

z : vertical coordinate measured from a reference level

b : channel width

C_c : contraction coefficient, equal to the ratio between the cross-section area A_B of the end section and the one A_A of the section A (Ferro 1999) in Figure 2.1. It is introduced for taking into account the convergence of the streamlines. Introducing

$C_c = \frac{A_B}{A_A} = \frac{y_e}{y_0}$ with constant channel width, into Equation 2.1 and by assuming horizontal bed one obtains,

$$\frac{Q}{b g^{1/2} y_0^{3/2}} = \frac{2\sqrt{2g}}{3 g^{1/2} y_0^{3/2}} \frac{y_e}{y_0} \left[H^{3/2} - (H - y_0)^{3/2} \right] \qquad (2\text{-}2)$$

Introducing $F_0 = \frac{Q}{b g^{1/2} y_o^{3/2}}$ into Equation 2.2

$$F_0 = \frac{2\sqrt{2}}{3} \frac{y_e}{y_0} \left[\frac{H}{y_0}^{3/2} - \left(\frac{H}{y_0} - 1 \right)^{3/2} \right] \qquad (2\text{-}3)$$

Finally, taking into account that

$$\frac{H}{y_0} - 1 = \frac{F_0^{\,2}}{2} \qquad (2\text{-}4)$$

From Equation 2.3 we obtain the following relationship for evaluating the ratio y_e/y_0

$$\frac{y_e}{y_0} = \frac{3F_0}{\left(2 + F_0^{\,2}\right)^{3/2} - F_0^{\,3}} \qquad (2\text{-}5)$$

Equation 2.5 for $F_0 = 1$ gives the classical result of Rouse (1936) as $y_e/y_0 = 0.715$ or $y_e/y_c = 0.715$.

Further the critical depth, which corresponds to the minimum specific energy is related to unit discharge through following equation:

$$y_c = \sqrt[3]{\frac{q^2}{g}} \qquad (2\text{-}6)$$

2.3 Dimensional Analysis

All the parameters involved are depicted in the same figure, Figure 2.1 and listed in Table 2.1 below:

Table 2.1 Parameters Involved in Dimensional Analysis

Parameter	Name	Dimension
y_e	Brink Depth	L
q	Discharge per Unit Depth	L^2/T
y_o	Uniform Flow Depth	L
b	Channel Width	L
S_o	Channel Bed Slope	-
g	The acceleration due to gravity	L/T^2
μ	Viscosity of water	M/LT
ρ	Density of water	M/L^3
n	Manning' s Roughness Coefficient	-

As implied by the sketch, the channel is assumed to be a rectangular prismatic channel. Furthermore, n, after Chow (1959), is assumed to be dimensionless.

The functional relationship of the kind:

$$y_e = f_1(q, y_o, b, S_o, g, \mu, \rho, n) \qquad (2\text{-}7)$$

Among these, parameters can be reduced to following form using Buckingham Π theorem with q, y_o, and ρ selected as the repeating variables;

$$\frac{y_e}{y_o} = f_2\left(\frac{q\rho}{\mu}, \frac{q}{y_o\sqrt{gy_o}}, \frac{y_o}{b}, n, S_o\right) \qquad (2\text{-}8)$$

where,

$$Re = \frac{q\rho}{\mu} \qquad (2\text{-}9)$$

and,

$$F_o = \frac{q}{y_o\sqrt{gy_o}} \qquad (2\text{-}10)$$

In other words,

$$\frac{y_e}{y_o} = f_3\left(Re, F_o, \frac{y_o}{b}, n, S_o\right) \qquad (2\text{-}11)$$

Furthermore, using the definition of y_c, the theoretical critical depth, stated in Equation 2.6, and the Buckingham Π theorem which states that product of Π terms are also Π terms, one obtains that;

$$\frac{y_e}{y_o}\times\left(\frac{q}{y_o\sqrt{gy_o}}\right)^{-2/3}=\frac{y_e}{y_o}\times\frac{y_o g^{1/3}}{q^{2/3}}=\frac{y_e}{y_c} \qquad (2\text{-}12)$$

Replacing y_e/y_0, the end depth ratio, by y_e/y_c, Equation 2.11 becomes,

$$\frac{y_e}{y_c}=f_4\left(Re,F_o,\frac{y_o}{b},n,S_o\right) \qquad (2\text{-}13)$$

Since,

$$F_o^{\,2}=\left(\frac{y_c}{y_o}\right)^3 \qquad (2\text{-}14)$$

Equation 2.11 can also be written in the following form;

$$\frac{y_e}{y_c}=f_5\left(Re,F_o,\frac{y_o}{y_c},n,S_o\right) \qquad (2\text{-}15)$$

During the experiments, the channel section has always been a wide rectangular channel. In other words, dependence of y_e/y_c on y_0/b could have not been observed. Therefore, y_0/b parameter has been dropped out of the equation. Furthermore, using the Manning's equation of the form;

$$V=\frac{\alpha}{n}R^{2/3}\sqrt{S_o} \qquad (2\text{-}16)$$

where α is a dimensional constant with a dimension of $LT^{-1/3}$ which assumes a value of unity in SI system, $\sqrt{S_0}/n$ can be discerned as another dimensionless entity of significant meaning. It must also be mentioned above here that all flows were

turbulent and dependence of y_e/y_c on Re number was not part of the scope of this thesis. Thus, equation can further be reduced to the following form:

$$\frac{y_e}{y_c} = f(F_o, \frac{\sqrt{S_0}}{n}, n,) \tag{2-17}$$

or,

$$\frac{y_o}{y_c} = f\ (\frac{y_o}{y_c}, \frac{\sqrt{S_0}}{n}, n,) \tag{2-18}$$

CHAPTER 3

EXPERIMENTAL STUDY

3.1 Description of the Experimental Set-up

The experiments were conducted in a metal rectangular flume 1.00 m in width and 12.06 m in length. Figure 3.1 shows the plan view of the channel. It had a steel bed and the sides of the channel were made of fiberglass. The base of the channel was made of well polished steel which represents smooth bed and later emery paper is glued to obtain rough bed. In Figure 3.2 the channel side view is shown. Since it is a big channel a steel structure is needed to prevent tilting and deformation at the bottom. The discharge measurements were made by a triangular weir (Figure 3.3). The weir capacity is enough to measure the maximum discharge used which is nearly 85 lt/s. The sloping bed is regulated by a screw. By the screw the channel can be adjusted to maximum slope of 1/9.22 and to maximum adverse slope of –1/41.80 .

Water, regulated by valves, was supplied from a constant head tank through two 20 cm pipes. Water issuing out from the channel was collected in a basin connected to a return channel. An energy dissipater is used at the base of the overfall to minimize the fluctuations caused by splashing resulting in a decrease in accuracy

of readings in the manometer measuring discharge. Additionally, screen type energy dissipater is used at the entrance of the channel in order to reach uniform flow.

The smooth channel was set to 9 different slopes 5 of them chosen to be nominally the same as the slopes used in the study of Turan (2002) to be able to compare the findings. The rough channel was set to 8 different slopes chosen in the criteria of nominally the same or near to slopes used in smooth channel in order to compare the results and to highlight the effect of roughness on flow characteristics. A point gauge mounted on rails along the channel allowed the normal depth, y_0, to be measured. Yet, there is another point gauge at the brink section allowed the brink depth, y_e, to be measured. In Figure 3.4 a cross sectional view of the channel demonstrating the gauge is given.

The depth of flow was determined with the accuracy of ±0.1 mm (equivalent of 0.1% precision). Measurements were taken for each of the preceding combinations of variables, provided that uniform flow was developed in the flume prior to the overfall.

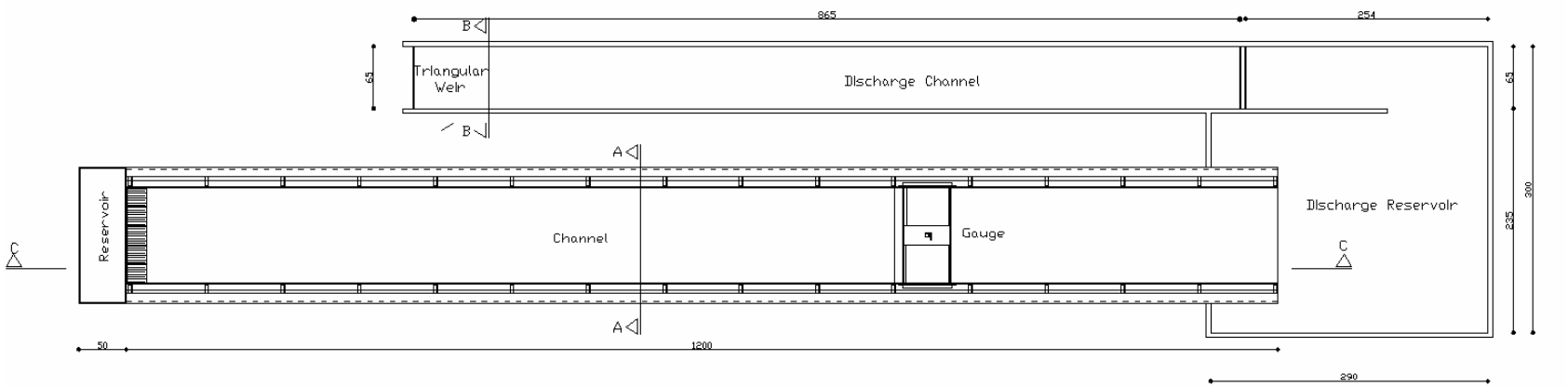

Figure 3.1 The Plan View of the Experimental Set up

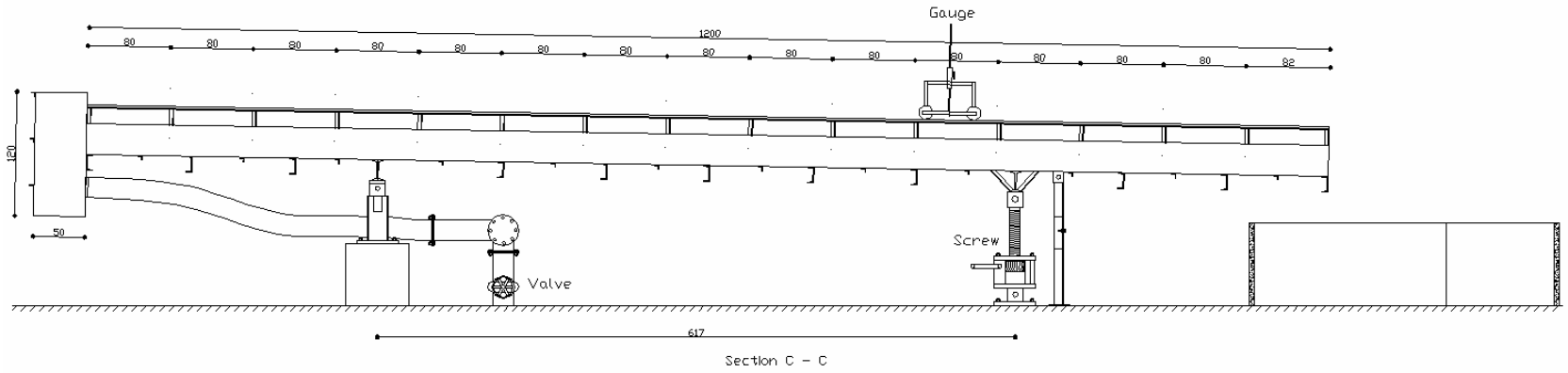

Figure 3.2 The Side View of the Experimental Set up

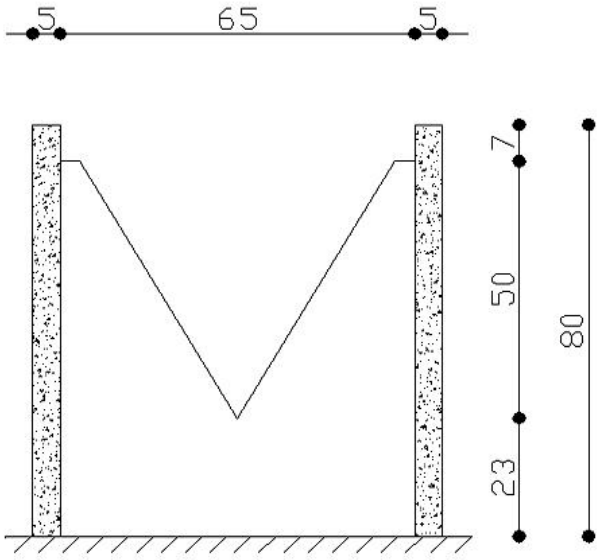

Figure 3.3 The Triangular Weir (Section B-B)

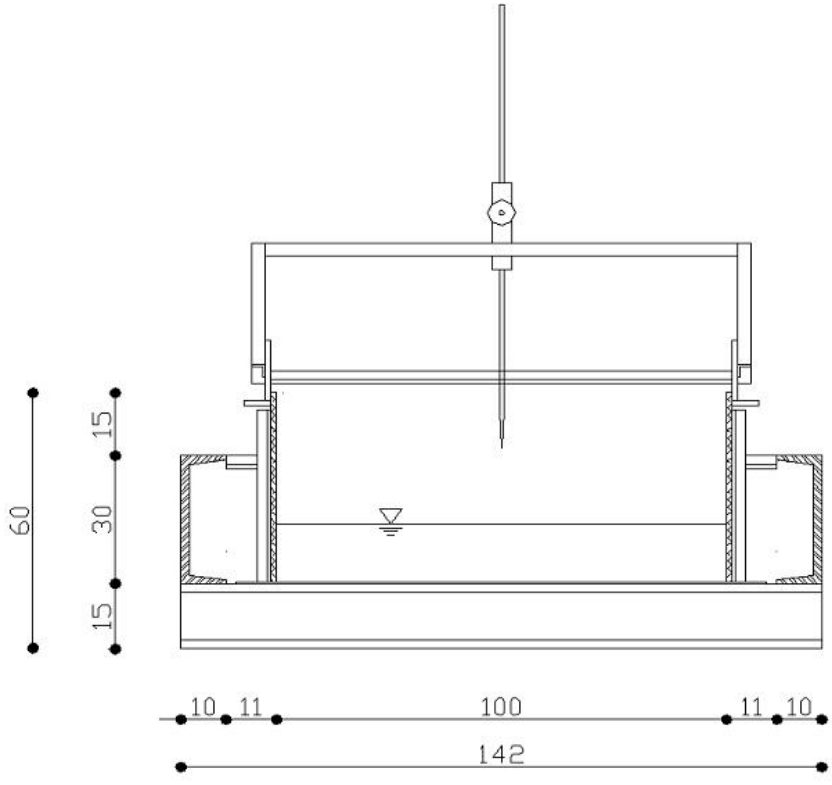

Figure 3.4 The Channel Section (Section A-A)

3.2 Discharge Measurements

The discharges were regulated with a valve at the supply pipe, and the rate of flow was measured by using a triangular weir, which has 60^0 notch angle. To check the calibration curve (Figure 3.8) for triangular weir, the basin at the downstream of the channel and a chronometer were used. The calibration curve is obtained from the experimental study of Gürsoy (2002),

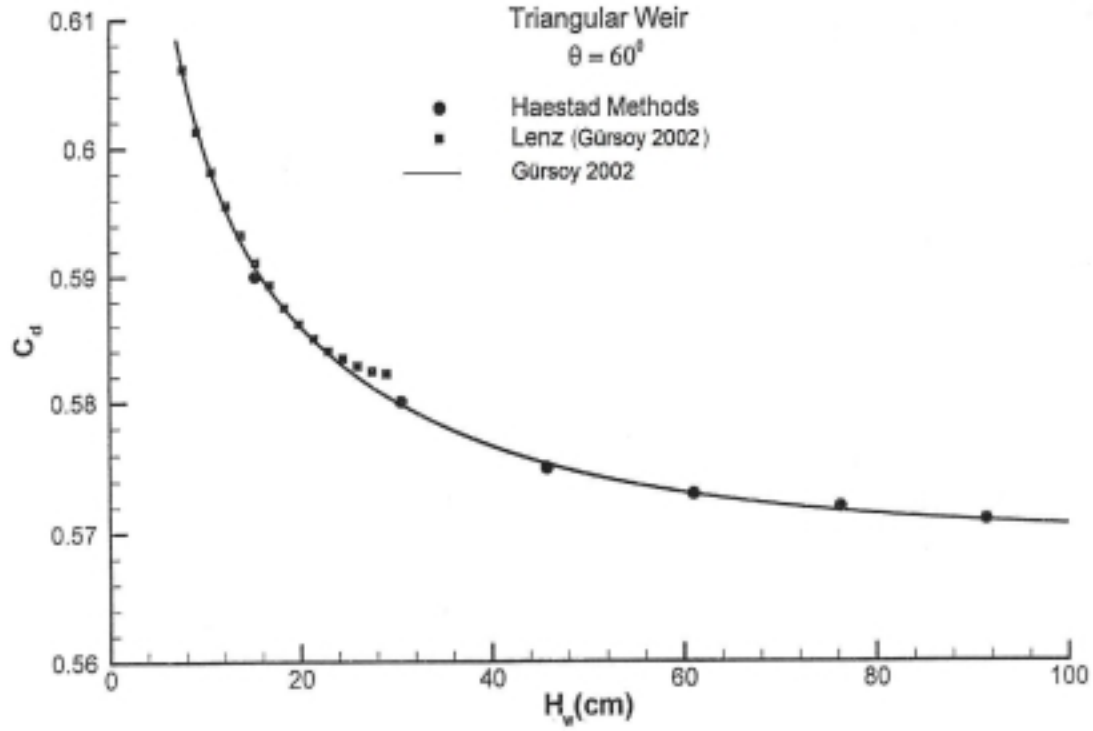

Figure 3.8 Triangular Weir Calibration Curve

where H_w is the head over the triangular weir and C_d is the weir coefficient. The calibration curve gives the following equation:

$$C_d = \exp\left(-0.385 - 0.0717\ln H_w + 0.00727(\ln H_w)^2\right) \qquad (3\text{-}1)$$

which will be used in the standard weir equation;

$$Q = C_d \frac{8}{15}\sqrt{2g}\tan\left(\frac{\theta}{2}\right)H_w^{5/2} \qquad (3\text{-}2)$$

These two equations are used in the calculation of discharge.

3.3 Measurements and Experimental Procedure

In each experiment, discharge, channel bottom elevations, water surface elevations and the brink depths were measured at the mid-point of the channel cross section. The data are given in Appendix-A.

At the beginning of the experimental study cross-waves were observed at the channel. These cross-waves were found to occur because of the irregularities at the channel bottom. This problem was solved by glazier's putty for the smooth channel. For each experimental set, the bottom and the slope of the channel were checked by level.

In each experiment, first the water was pumped to a tank in order to achieve a constant head. The discharge amount was adjusted by the valves on the supply pipes, which were connected to the constant head tank. By changing the opening of valves at the supply pipe, various values of discharges and hence Froude numbers were obtained. From the supply pipes water entered to the channel through a small basin by which some of its energy is dissipated. The readings were recorded after a period of time in order to gain steady flow conditions.

The normal depth measurements were made normal to the channel bottom by a point gauge. The measurements were started from 6 m away from the brink section

and continued at points where the locations were determined before, in the procedure of finding the optimum location of normal depth that will be discussed in Section 3.4, to the brink section. By these measurements it was found that uniform flow condition is obtained at the channel.

In order to measure the brink depths another point gauge which was parallel to the gravity was used at the brink section. The measurement of the gauge measuring the normal depths was perpendicular to the channel bottom so a geometrical correction was performed to achieve normal depth values parallel to the gravity direction. From the channel the water discharged to a stilling basin and from this stilling basin it ran out to the return channel. The discharge of the experiment set was measured by the triangular weir on the return channel.

At the end of each experiment set the bed slope S_0, the normal depth y_0 , the brink depth y_e , and the discharge Q values were measured.

3.4 Procedure of Data Collecting

In the present study in every experimental set brink depth, normal depth and discharge were measured. The flow rate and the brink depth were measured straightforward since the points and the procedure are obvious. The challenging phenomenon was determination of points where normal depth develops. For this reason, in the first runs where data for smooth bed conditions were collected, the number of recorded points on the horizontal axis of the channel bed and their spacing were chosen to be enough to give the correct coordinates of normal depth. For smooth channel, the correlation between the depths at points ranging from 550 cm distant from the brink section to 170 cm away from the brink section was calculated in order to find out the optimum location for normal depth. The points, which have the minimum variance to the average of depths from 550 cm to 170 cm, gave the

optimum points where normal depth developed. After determining the point of the normal depth the number of points data collected was decreased by measuring the depths only on the selected points. Instead, increasing the number of readings at the optimum location of normal depth had yielded an improvement in the accuracy. The same strategy was followed for rough channel experiment sets.

The correlation of the values of points where normal depth is expected to develop is given in Figures 3.9 and 3.10. The root mean squares of the normal depth readings to the average of the readings in the range of aforementioned points with the horizontal location of them are given in Figure 3.9 for smooth channel and Figure 3.10 for rough channel. From the figures below the optimum locations came out to be at x_1=450 cm, x_2=240 cm, x_3=260 cm for smooth channel. The normal depth was the average of depths measured at these three. For rough channel the point which gave the least root mean square value was x_1=450 cm, therefore in the last 4 slope runs the normal depth readings were collected at this point.

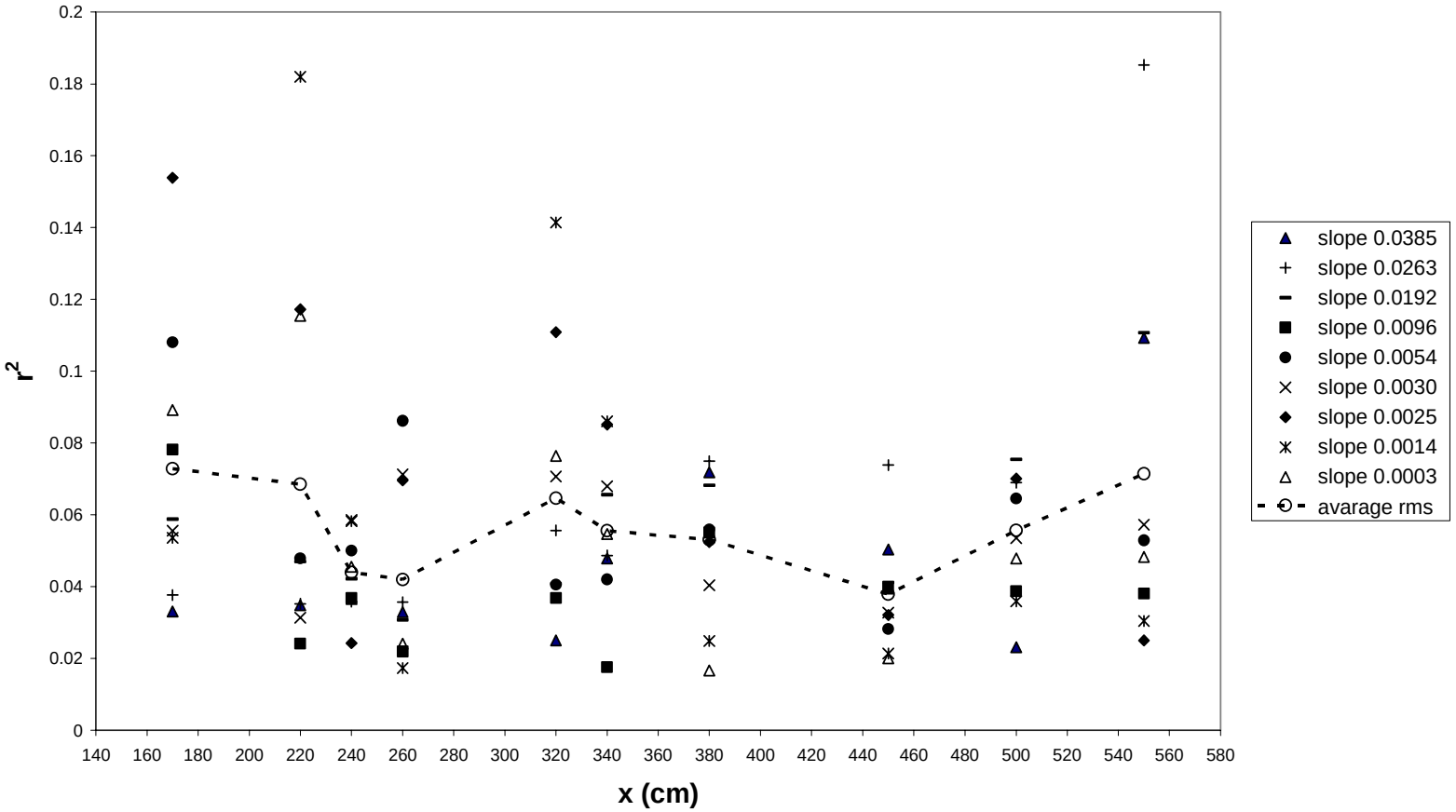

Figure 3.9 Finding Optimum Location of Normal Depth for Smooth Channel

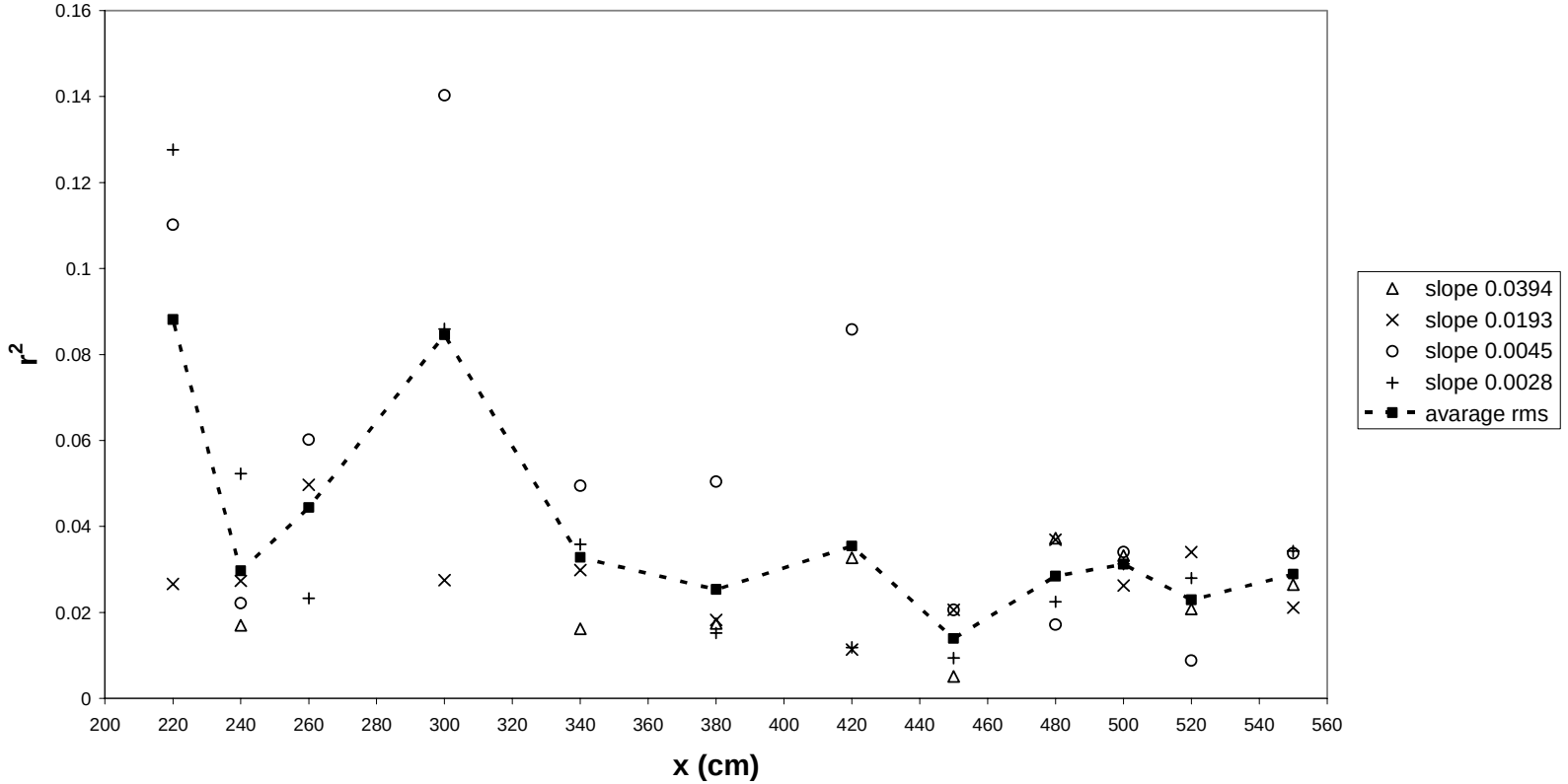

Figure 3.10 Finding Optimum Location of Normal Depth for Rough Channel

In order to ensure that the characteristic of the free overfall is a function of discharge, slope and roughness, the channel length should be long enough. Cartens and Carter (1955) (in Bauer and Graff (1971)) suggested that the channel length should be at least 20 times greater than the critical depth. During the experiments maximum critical depth is observed around 0.09 m. Therefore the uniform flow measurements 2 m away from the brink will be safe.

In each experimental set after the valves were opened accordingly a sufficient time interval was waited to let the flow be steady. The water depth measurements were made then. When a discharge is fixed on the channel, readings for a complete set were repeated five times in order to decrease the effect of flow trends that may cause small fluctuations on discharge. Repetition of readings would also check the accuracy of the operator. The maximum and the minimum values recorded were cancelled and the mean value of the remaining three was the depth of that point. The same procedure was applied for the readings of the head occurred at the weir to minimize the trend effect on discharge measurements.

The basic strategy through all calculations was checking the validity and correctness of a calculation by crosscheck calculations. The measured normal depth was compared with the normal depth calculated from Manning's equation by an iterative solution where discharge and Manning's roughness coefficient were input for the equation. The results are discussed in Appendix-B.

CHAPTER 4

DISCUSSION OF RESULTS

4.1 Experimental Findings

The experiments for smooth bed were performed for 9 slopes, namely of 0.0003, 0.0014, 0.0025, 0.0030, 0,0054, 0.0096, 0.0192, 0,0263 and 0.0385. For the range of discharges covered in the study, of the 82 experiments run for smooth bed, 19 were in subcritical regime and 63 were in supercritical regime. In the same manner for rough channel, there were 8 slopes, namely of 0.0008, 0.0023, 0.0028, 0.0045, 0.0088, 0.0193, 0.0269 and 0.0394 used. There were total of 48 experiments run with rough bottom of which 25 were in subcritical regime. The total number of experiments conducted, were 130. The Froude numbers range that was obtained by the experiments was 0.42 to 3.68 and the discharge range was 1.61 lt/s to 84.12 lt/s.

4.2 Determination of Manning's Roughness Coefficient

The estimation of roughness coefficient and hence discharge capacity in a channel or in a river is one of the most fundamental problems facing in river engineering. Without an accurate estimate of conveyance, very little confidence can

be placed in subsequent design calculations or predictions. Frequently, little or no field data are available especially for flood flows; therefore the engineer must estimate a roughness value and apply to the river in question to obtain a stage-discharge relationship as a basis for further design calculations. This experimental study is performed in the light of the importance of determination of the effect of roughness on flow behavior.

In order to achieve the correct value of Manning's roughness coefficient, n, for the channel, the Manning equation is used. Recalling Equation 2.16 for SI system,

$$V = \frac{1}{n} R^{2/3} S^{1/2} \qquad (4\text{-}1)$$

where R is the hydraulic radius $R = \frac{A}{P}$ and P is the wetted perimeter and A is the flow area, S is the slope of the energy grade line, which is taken identical to the channel bottom slope in uniform flow.

Since the normal depth and discharge values are measured for all the slopes tested for both smooth and rough channel, the only unknown in Equation 4.1 is the Manning's n. In Figure 4.1 the slopes of the best-fit lines give the Manning's n values for smooth and rough bed. The average value $\bar{n}$ for smooth channel is equal to 0.0091.

Following the same approach the average value $\bar{n}$ for rough channel is equal to 0.0147 deduced from Figure 4.1. Therefore, in this experimental study the Manning's n values will be used as 0.0091 for smooth channel, and 0.0147 for rough channel.

In determination of n, the values measured in mildest slopes were not included in the calculations due to the invalidity of Manning's Equation on horizontal or nearly horizontal channels.

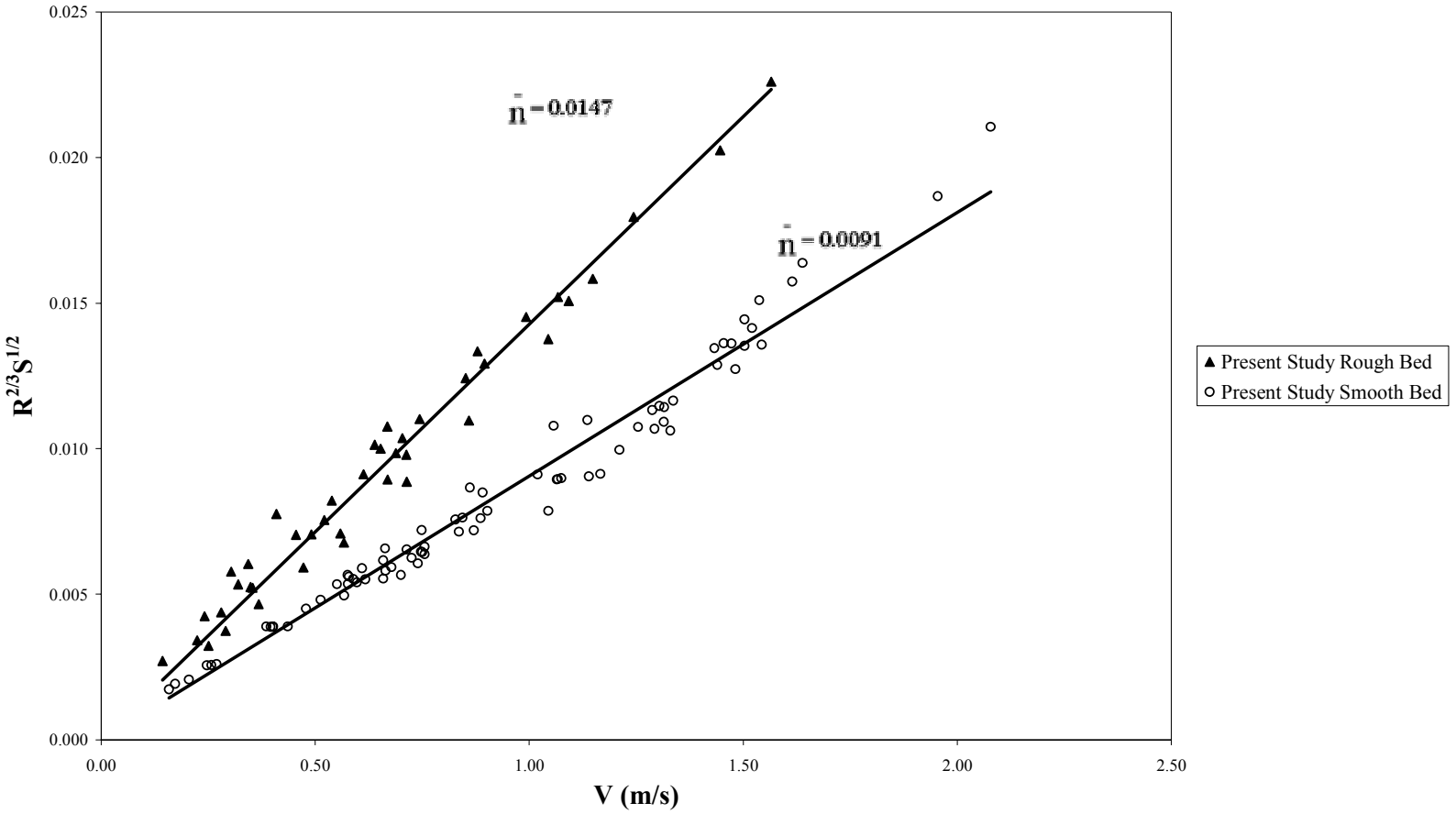

Figure 4.1 Determination of Manning's Roughness Values

4.3 The y_e/y_c Values for the Slopes Tested

Brink Depth y_e, is usually taken as vertical to the cross-section. However in some studies it is not well reported. In the present study the brink depth and normal depth values are taken to be parallel to the gravity direction. This approach will be more suitable for field applications.

The relationship between y_e and y_c for smooth channel and rough channel are presented in Figure 4.2a and Figure 4.2b respectively. The best-fit lines shown have been fitted through the data for each slope tested. The slope of the best-fit lines gives the ratio of y_e/y_c. As it is seen in Figure 4.2a for smooth channel for the slopes of 0.0385, 0.0263, 0.0192, 0.0096, 0.0054, and 0.0030 the y_e/y_c values increases. The lowest value occurs at 0.0385 and the highest value occurs at 0.0030. For these 6 slopes the flows are in supercritical flow condition. As it is seen in Figure 4.2a, the y_e/y_c value for 0.0025 is lower than the y_e/y_c value for 0.0030. This is a result of the change at the flow condition since the flow at slope 0.0025 is in subcritical flow condition. Furthermore, slopes stating subcritical flow condition show an increasing trend in y_e/y_c values with decreasing slope. After the same analysis deducted from Figure 4.2b, for rough channel for the slopes that are in subcritical flow condition and supercritical flow condition separately, a similar result had appeared; as slope decreases, y_e/y_c values increase. For the slopes tested, the coefficients of the best-fit lines placed through the data of smooth and rough channel are given in Table 4.1, together with their root mean square values, r^2.

Comparing the values of slopes of smooth channel with nominally same slope constructed for rough channel gives an outcome of a sentence; as roughness increases y_e/y_c values increase. In order to verify this deduction analyzing an example from Table 4.1 result in; y_e/y_c value for smooth channel slope is less than the y_e/y_c value for the nominally same slope for rough channel.

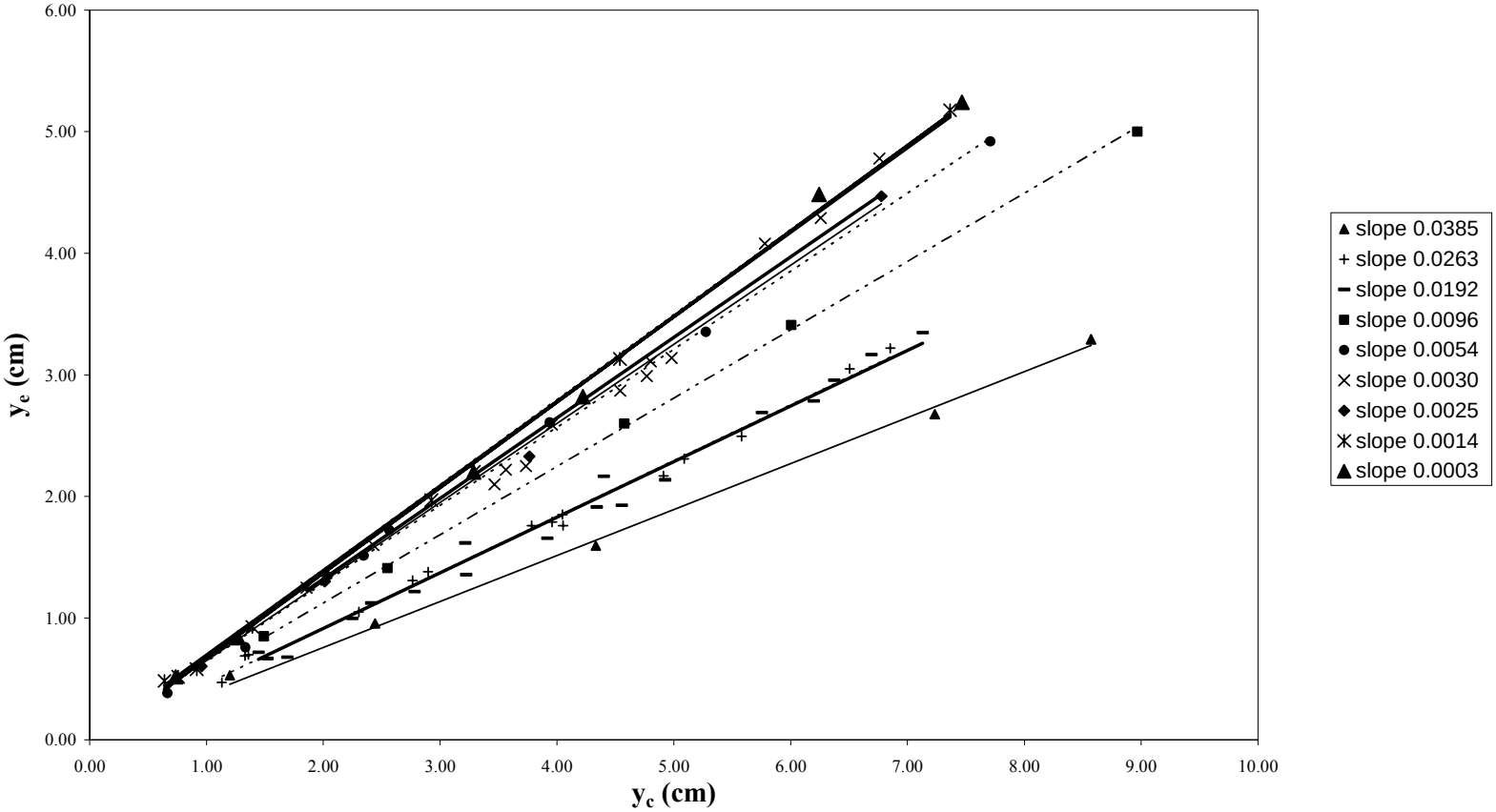

Figure 4.2a Relationship between y_e and y_c with Best-Fit Lines for Each Slope Tested for Smooth Channel

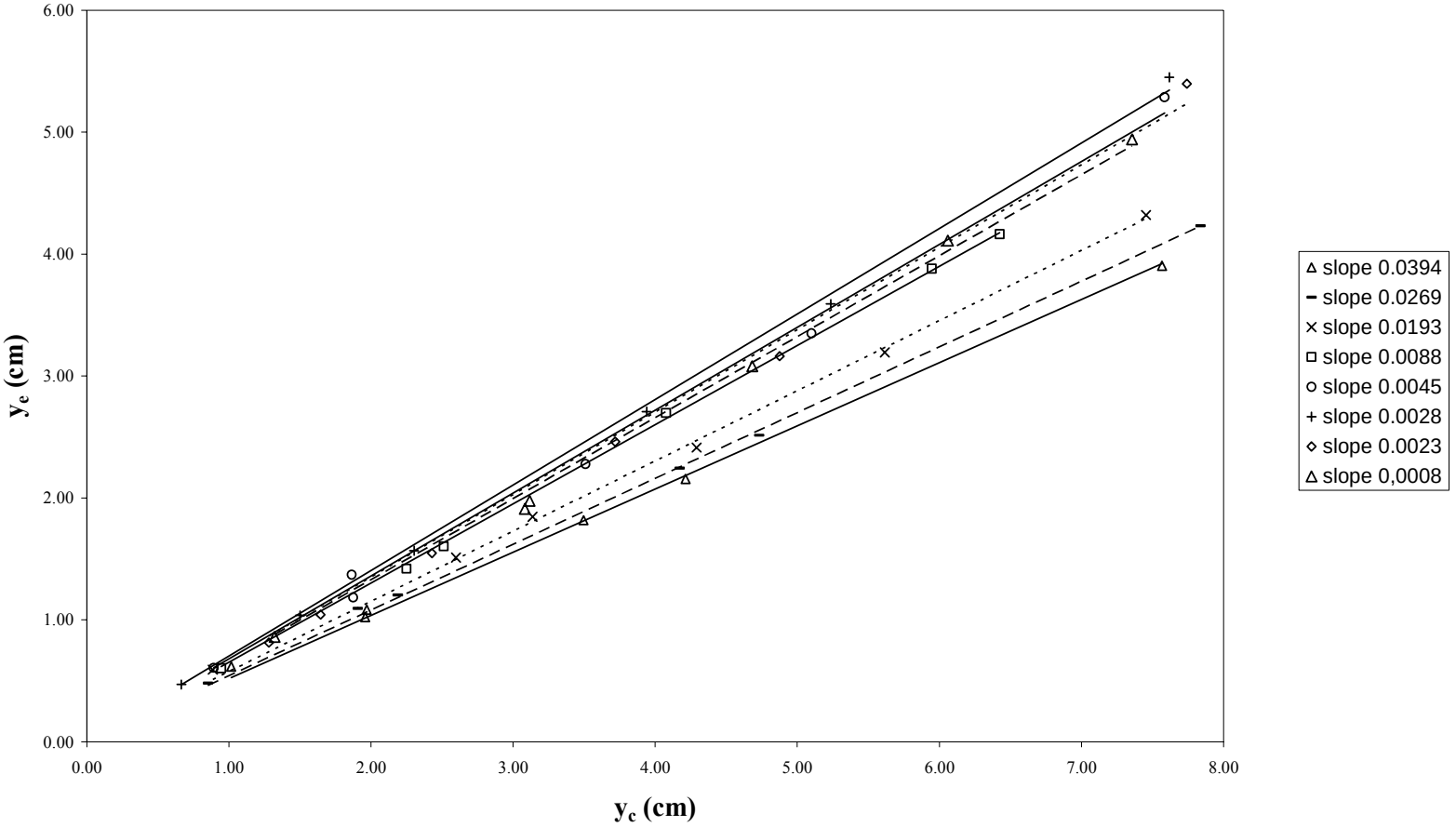

Figure 4.2b Relationship between y_e and y_c with Best-Fit Lines for Each Slope Tested for Rough Channel

Table 4.1 Best Fit y_e/y_c Values and Corresponding r^2 Values Obtained

Slope	State of Surface	y_e/y_c	r^2	State of Flow
0.0394	Rough	0.5181	0.9982	Supercritical
0.0385	Smooth	0.3782	0.9972	Supercritical
0.0269	Rough	0.5396	0.9993	Supercritical
0.0263	Smooth	0.4588	0.9946	Supercritical
0.0193	Rough	0.5755	0.9984	Supercritical
0.0192	Smooth	0.4573	0.9874	Supercritical
0.0096	Smooth	0.5616	0.9996	Supercritical
0.0088	Rough	0.6501	0.9995	Supercritical
0.0054	Smooth	0.6418	0.9983	Supercritical
0.0045	Rough	0.6800	0.9959	Subcritical
0.0030	Smooth	0.6618	0.9729	Supercritical
0.0028	Rough	0.7016	0.9986	Subcritical
0.0025	Smooth	0.6504	0.9979	Subcritical
0.0023	Rough	0.6760	0.9956	Subcritical
0.0014	Smooth	0.6956	0.9992	Subcritical
0.0008	Rough	0.6644	0.9966	Subcritical
0.0003	Smooth	0.6990	0.9976	Subcritical

4.4 Variation of y_e/y_c with $\sqrt{S_0}$

S_0 is one of the dimensionless parameters. Following Alastair et al. (1998), the relationship between y_e/y_c and $\sqrt{S_0}$ is investigated. The best-fit line coefficients of y_e/y_c values for both smooth and rough channel are plotted against $\sqrt{S_0}$ values. In Figure 4.3 the y_e/y_c and $\sqrt{S_0}$ variation for smooth channel (n=0.0091), and for rough channel (n= 0.0147) are shown. In this figure the supercritical values are used (Slope ranges between 0.0385 to 0.0030 for smooth channel and 0.0394 to 0.0088 for rough channel) since the behavior changes for subcritical cases.

The increasing influence of roughness with slope can clearly be seen in Figure 4.3; the quadratic best-fit lines diverge as the slope increases and best-fit line coefficients of y_e/y_c values appear to increase with increasing roughness. As a result of Figure 4.3 the relationships given in tabular form Table 4.2, below is achieved:

Table 4.2 Best Fit Equations and Corresponding r^2 Values Obtained

Equation No	Slope Range	n	Equation	The root mean square r^2
4-2	0.0385~0.0030	0.0091	$\frac{y_e}{y_c} = 0.77 - 2.05\sqrt{S_0}$	0.9708
4-3	0.0394~0.0088	0.0147	$\frac{y_e}{y_c} = 0.76 - 1.29\sqrt{S_0}$	0.9604

Figure 4.3 indicate that there is an influence of Manning's n value on the dispersion of the values leading the study to analyze the relationship between y_e/y_c

values with $\sqrt{S_0}$ /n to decrease the dependency of y_e/y_c values to Manning's n resulting in a single design curve.

It should be noted that the coefficients in Equations 4.2 and 4.3 are the rounded values for the sake of convenience. The original values of coefficients are given in Appendix-A.

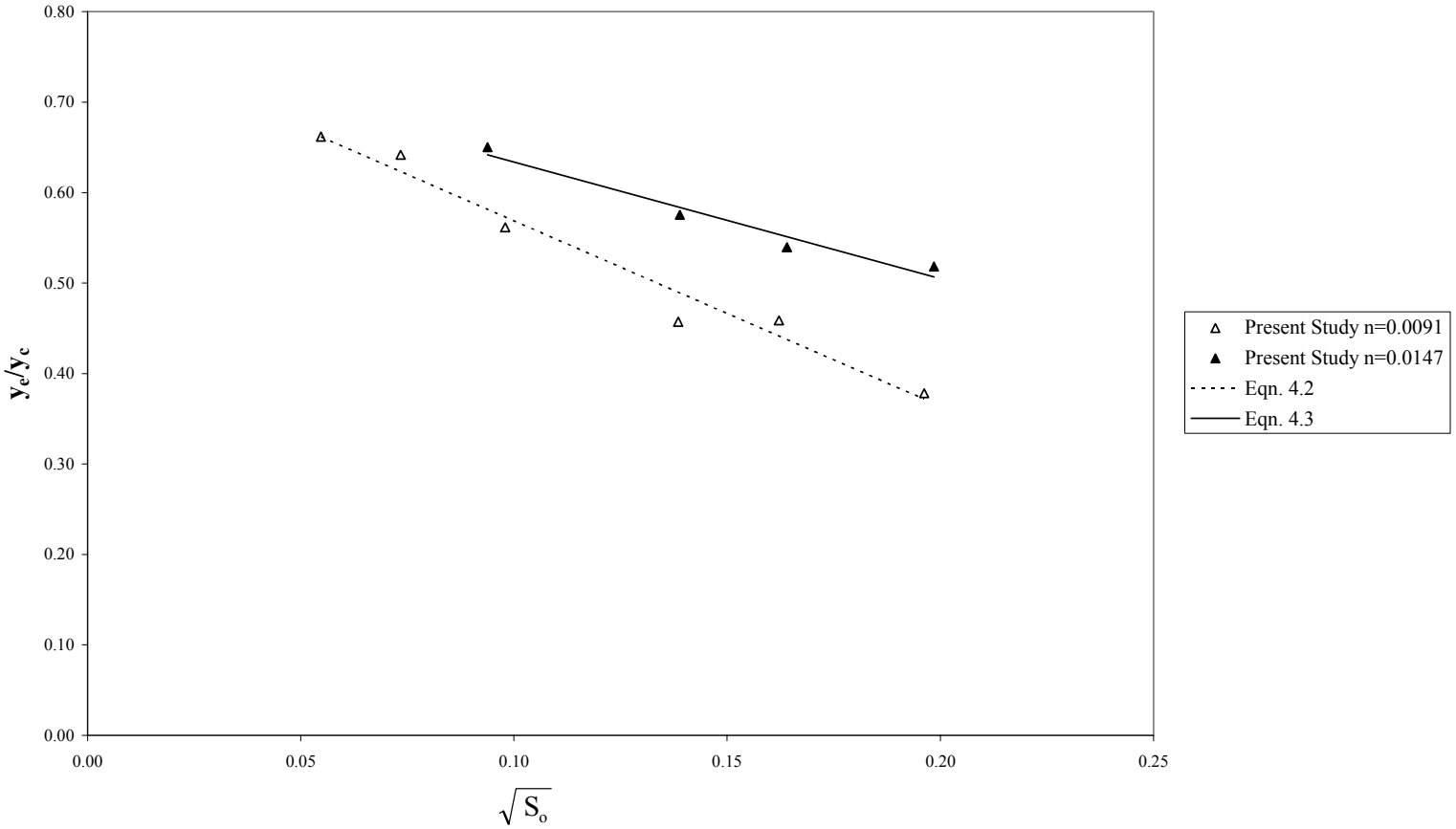

Figure 4.3 Variation of y_e/y_c with $\sqrt{S_0}$ for the Present Study

4.5 Variation of y_e/y_c with $\frac{\sqrt{S_o}}{n}$

The relationship between y_e/y_c with $\sqrt{S_0}$, as depicted in Figure 4.3, suggests that $\sqrt{S_0}$ /n as it is a dimensionless parameter in equation, might be a better variable to explain variation of y_e/y_c. This relationship is shown in Figure 4.4. The deduction to be underlined from Figure 4.4 would be the similarity trend of both smooth and rough bed values leading the study to a single design curve and equation for discharge prediction with known S_o and n. Hence, the best-fit line of the combined data of smooth and rough bed ends up with a relationship, in which the effects of channel slope and bed roughness are aggregated. This relationship with combined data of smooth and rough bed is given below:

$$\frac{y_e}{y_c} = 0.76 - 0.02\frac{\sqrt{S_0}}{n} \qquad (4\text{-}4)$$

The root mean square, $r^2 = 0.9654$

It should be noted that the coefficients in Equation 4.4 are the rounded values. The original values of coefficients are given in Appendix-A.

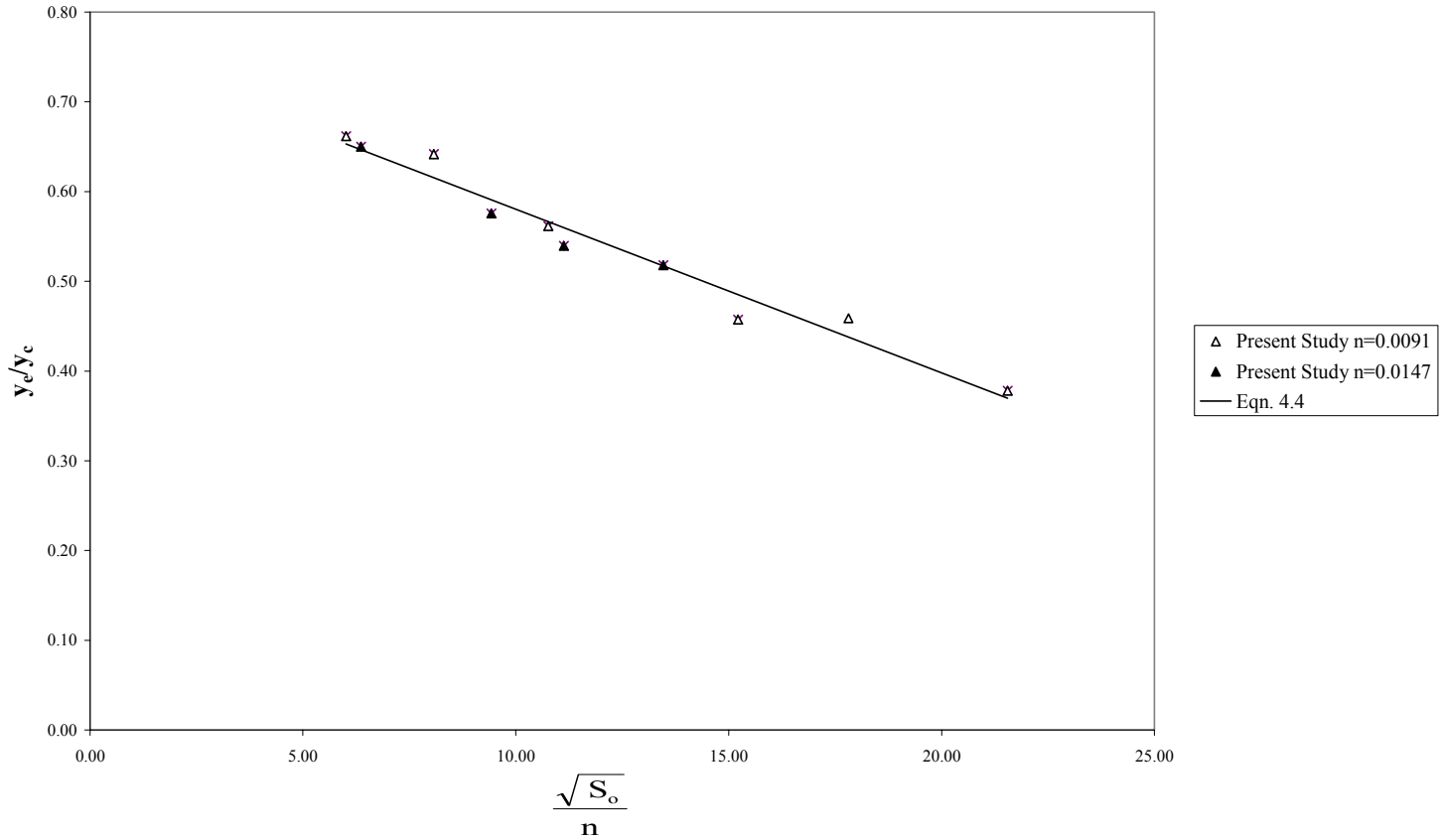

Figure 4.4 Variation of y_e/y_c with $\frac{\sqrt{S_o}}{n}$ for the Present Study

4.6 Comparison of the Present Study with Earlier Studies

The results of the present study are compared with the results of Alastair et al. (1998) and Turan (2002). Table 4.3 shows the slopes range and Roughness values for all three studies that will be compared.

Table 4.3 Slope Range and Roughness Values

Researcher	Slope Range		n	
	Smooth	Rough	Smooth	Rough
Alastair	0.0333 to 0.0033	0.0333 to 0.0100	0.0099	0.0147
Turan	0.0400 to 0.0033	-	0.0100	-
Present Study	0.0385 to 0.0030	0.0394 to 0.0088	0.0091	0.0147

In Figure 4.5 the variation of y_e/y_c and $\sqrt{S_0}$ /n of the present study for smooth channel, and the present study for rough channel are given. In this figure the supercritical values are used (slope ranges between for smooth channel and 0.0394 to 0.0088 for rough channel) since the behavior changes for subcritical cases. Also in Figure 4.5 the same variation is given for the study of Alastair et al. (1998), and for Turan (2002), which studied only in smooth channel. It is seen that the smooth bed values of supercritical cases of Alastair et al. (1998), Turan (2002) and the present study's results are in good agreement. As seen in Figure 4.5 the y_e/y_c values of smooth channels of Alastair et al. (1998) and Turan (2002) are slightly higher than the present study. The difference between dispersion of y_e/y_c values for both smooth beds is due to the reason that Alastair et al. (1998) and Turan (2002) used a higher Manning's n value. It can be deduced from comparing the present study of rough bed and the one of Alastair et al. (1998) that; the rough bed values of Alastair et al. (1998) and the present study give similar results. The scattering of y_e/y_c values for

rough bed converge slightly as slope reaches its steepest values. Main cause of this difference is the side effect since Alastair et al. (1998) used a channel of 0.30 m width. The secondary and common cause for both Alastair et al. (1998) and the present study is at high flow rates, it is estimated that fluctuations in the weir manometer measuring the discharge, which is a consequence of hardly achieved steady state conditions, could easily result in a 2% error or more in the discharge and, therefore, a corresponding error in the computed y_c. These possible inaccuracies, combined with the lack of accuracy of the point gauge depth readings at the higher flow rates which mostly occurred in steeper slopes, could explain the apparent convergence seen in Figure 4.5 at steeper slopes.

In order to corroborate the perceptible conformity of the present study and earlier studies root mean squares of studies to the design curve of the present study. The root mean square of the combined y_e/y_c values of the present study to the design curve is 0.0165 where the one of the combined data of Alastair et al. (1998) and Turan (2002) is 0.0426. In addition, the correlation of the present study is 0.9825 and the one of abovementioned studies is 0.9716, which are considered to be relatively high. These statistical projections validate the reasonable agreement between the present study and the studies of Alastair et al. (1998) and Turan (2002).

As a consequence, the present study is in verification with the abovementioned earlier studies.

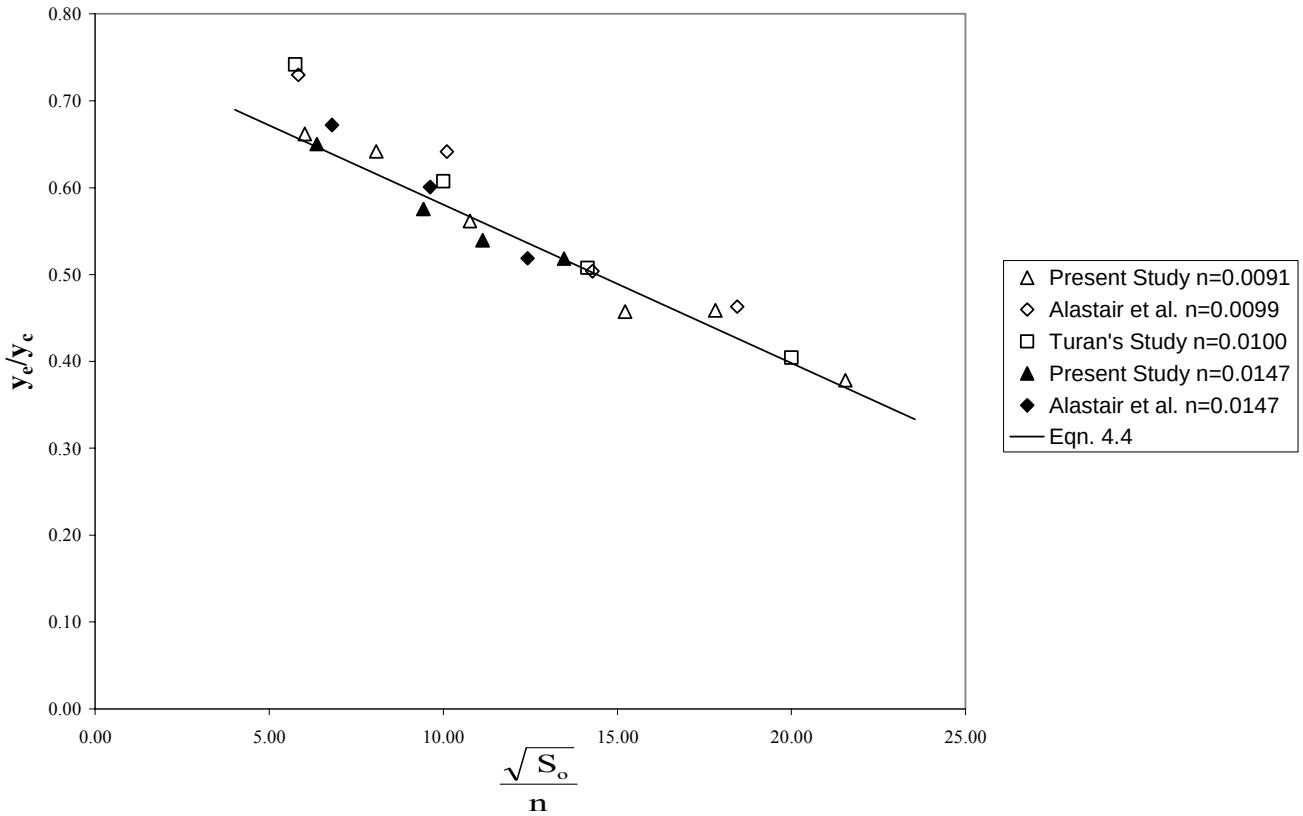

Figure 4.5 Variation of y_e/y_c with $\frac{\sqrt{S_o}}{n}$ for Comparing Present Study to the Data of Alastair et al (1998). and Turan (2002)

4.7 Variation of y_e/y_c with F_o^2

As y_e/y_c is influenced by S_0 and n, a function was sought that encompasses these variables. Upstream Froude Number, F_0, is influenced by S_0 and n. Figure 4.6 and Figure 4.7 show y_e/y_c plotted against F_0^2. In Figure 4.6 y_e/y_c values of each slope tested with bed conditions are given with their corresponding F_0^2 values. In demonstrating graphs F_0^2 is used because discharge is directly related to $F_0^{2.}$ Another reason to use F_0^2 would be to illustrate the values of y_e/y_c of slopes with corresponding roughness more discrete. Furthermore, the reason why the axis of F_0^2 is in logarithmic scale is to show the dispersion of subcritical and supercritical values separately. As a result of Figure 4.6 and 4.7 the most important deduction that can be stated would be that subcritical flows trend a linear distribution where the supercritical flow conditions disperse in an exponential trend. Furthermore, comparing y_e/y_c values of slopes for smooth bed with the nominally the same slopes for rough bed yields; roughness shifts the orientation of values of y_e/y_c and F_0^2 on the same trend formed by slopes. Consequently, roughness does not change the trend of distribution of y_e/y_c values and F_0^2 but shifts the placement on a single trend line.

It should be noted that the forming best fit lines of these dispersion of y_e/y_c values versus F_0^2 values are useless in calculating y_e/y_c to predict discharge (as they require discharge to be known), and are only included here to verify the reason of form and usage of Figure 4.4.

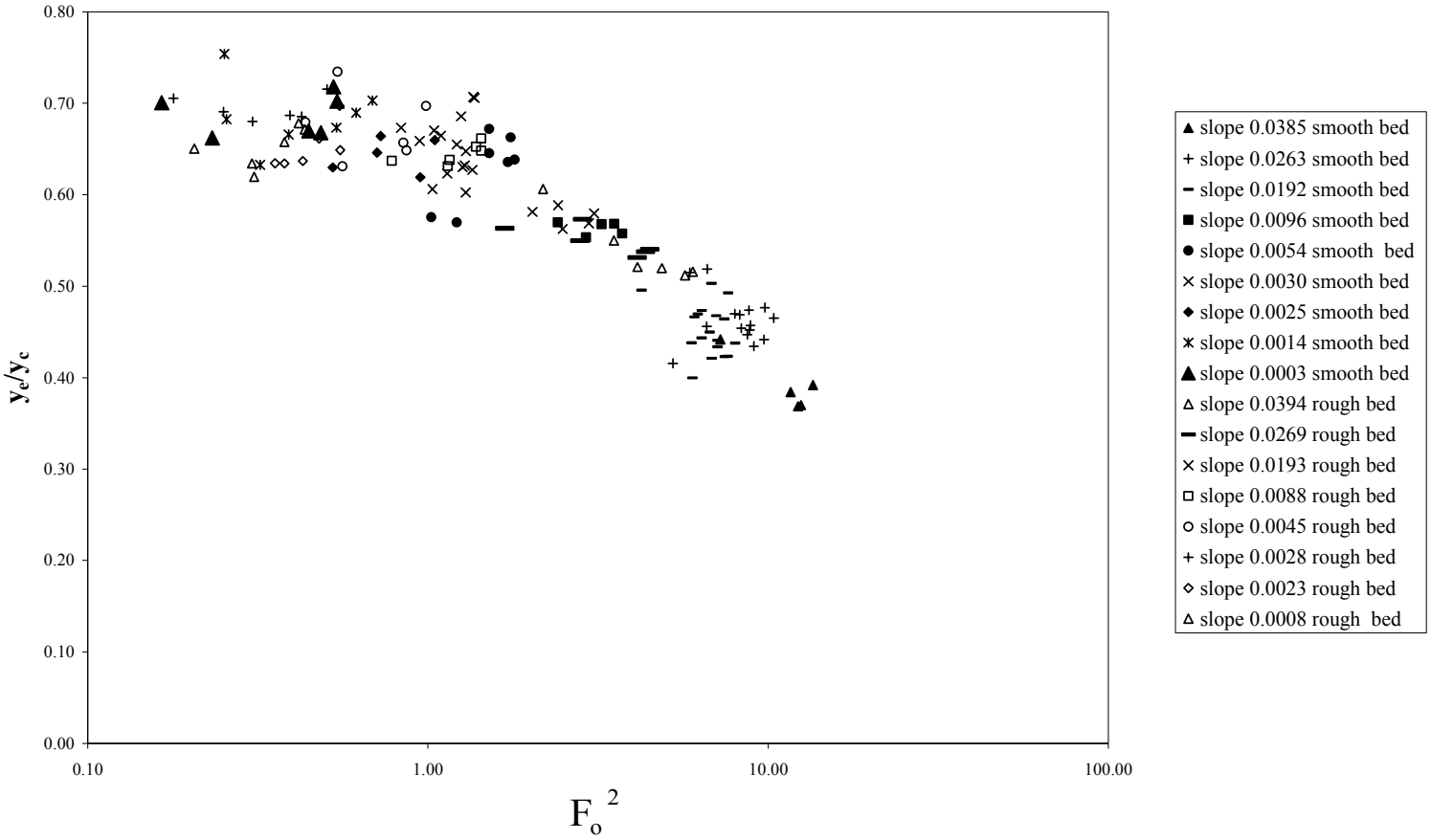

Figure 4.6 Variation of y_e/y_c with F_0^2 for Slopes of the Present Study

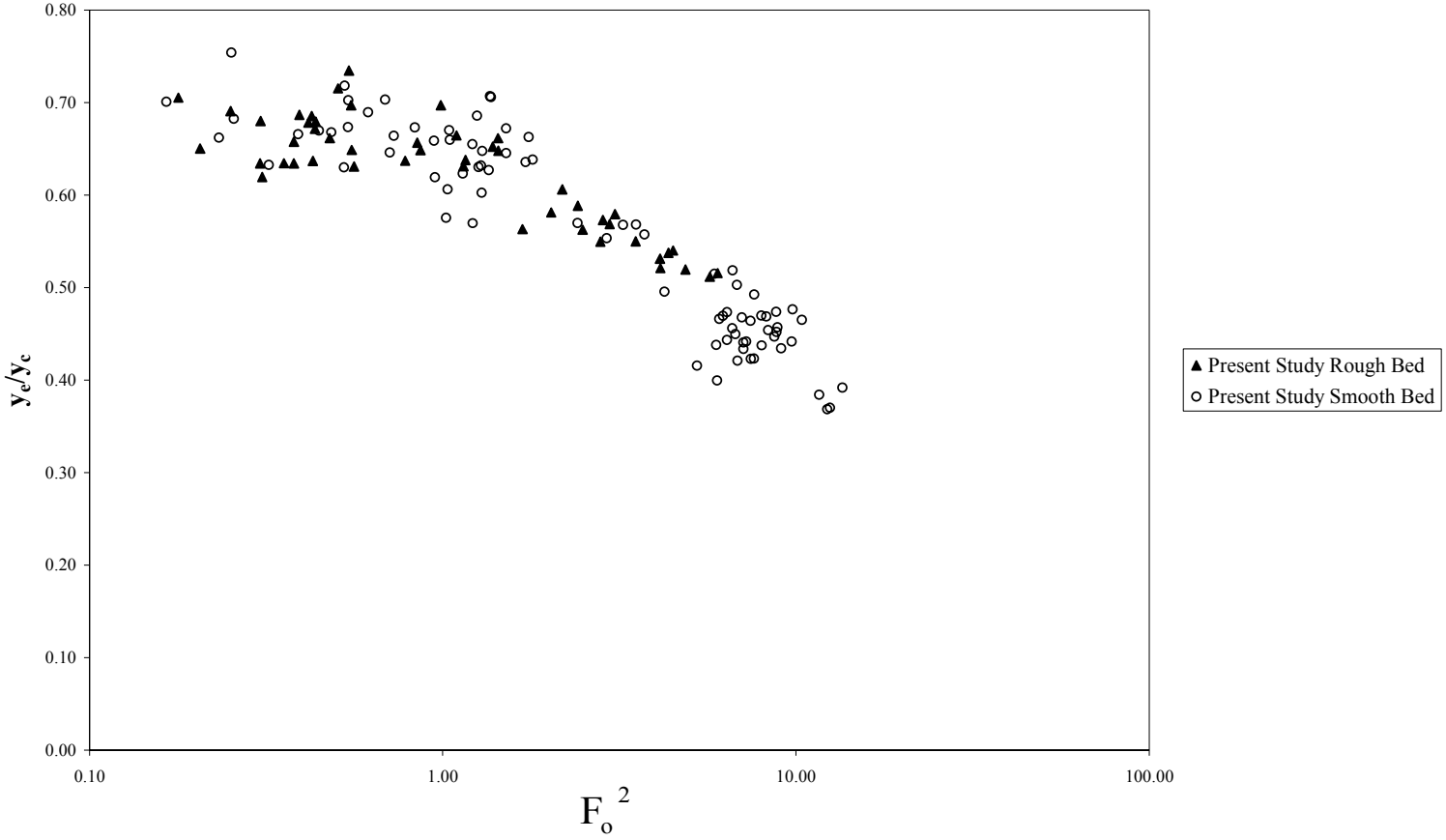

Figure 4.7 Variation of y_e/y_c with F_0^2 for Smooth and Rough Beds of the Present Study

4.8 Variation of y_e/y_c with y_0/y_c

As a result of dimensional analysis it is shown that y_e/y_c may be related to y_0/y_c. It will be a practical way of discharge measurement if the engineer measures the discharge only by knowing y_e and y_0. This is an alternative solution to predict discharge with different input data. Since both of the parameters include y_c, iteration is needed to calculate discharge. This relationship is given in Figure 4.8 and in Figure 4.9. In Figure 4.8 y_e/y_c values with corresponding y_0/y_c values of the present study with both smooth and rough bed conditions are given. In Figure 4.9 the dispersion of the values of smooth and rough bed values are given. As it is seen in Figure 4.9 the rough bed and smooth bed values illustrate the same trend. In addition, inferring from Figure 4.8, the values of a slope of rough channel differs from the values of a nominally the same slope of smooth channel, showing dispersion on the same trend line but shifted. It can also be deduced from Figure 4.8 and 4.9, the spreading of subcritical values that of y_0/y_c values greater than or equal to 1, is linear which is reported also by Bauer and Graf (1971) and Kraijenhof and Dommerholt (1977). However the distribution of supercritical values that of y_0/y_c values less than 1, is polynomial and first reported in the present study. Therefore, combining the values of smooth and rough channel yields a conditional relationship given below:

$$\frac{y_e}{y_c} = -0.51\left(\frac{y_0}{y_c}\right)^3 - 0.36\left(\frac{y_0}{y_c}\right)^2 + 0.83\left(\frac{y_0}{y_c}\right) \qquad \text{For} \quad \frac{y_0}{y_c} < 1 \qquad (4\text{-}5)$$

$$\frac{y_e}{y_c} = 0.67\left(\frac{y_0}{y_c}\right) \qquad \text{For} \quad \frac{y_0}{y_c} \geq 1 \qquad (4\text{-}6)$$

For Equation 4.5 The root mean square, $r^2 = 0.9275$

As it seen from the above equations for the critical flow where $y_0/y_c = 1.00$, the value of y_e/y_c yields to 0.67, and also the peak point of the equation occurs where $y_0/y_c = 1.00$ representing the critical flow. The supercritical values, that are the values satisfying the condition $y_0/y_c > 1.00$, disperse linearly as inferred from Figure 4.8. In summary, Equation 4.5 and 4.6 contain 3 phases of flow as supercritical, critical and subcritical flow.

It should be noted that the coefficients in Equation 4.5 and 4.6 are the rounded values. The original values are given in Appendix-A.

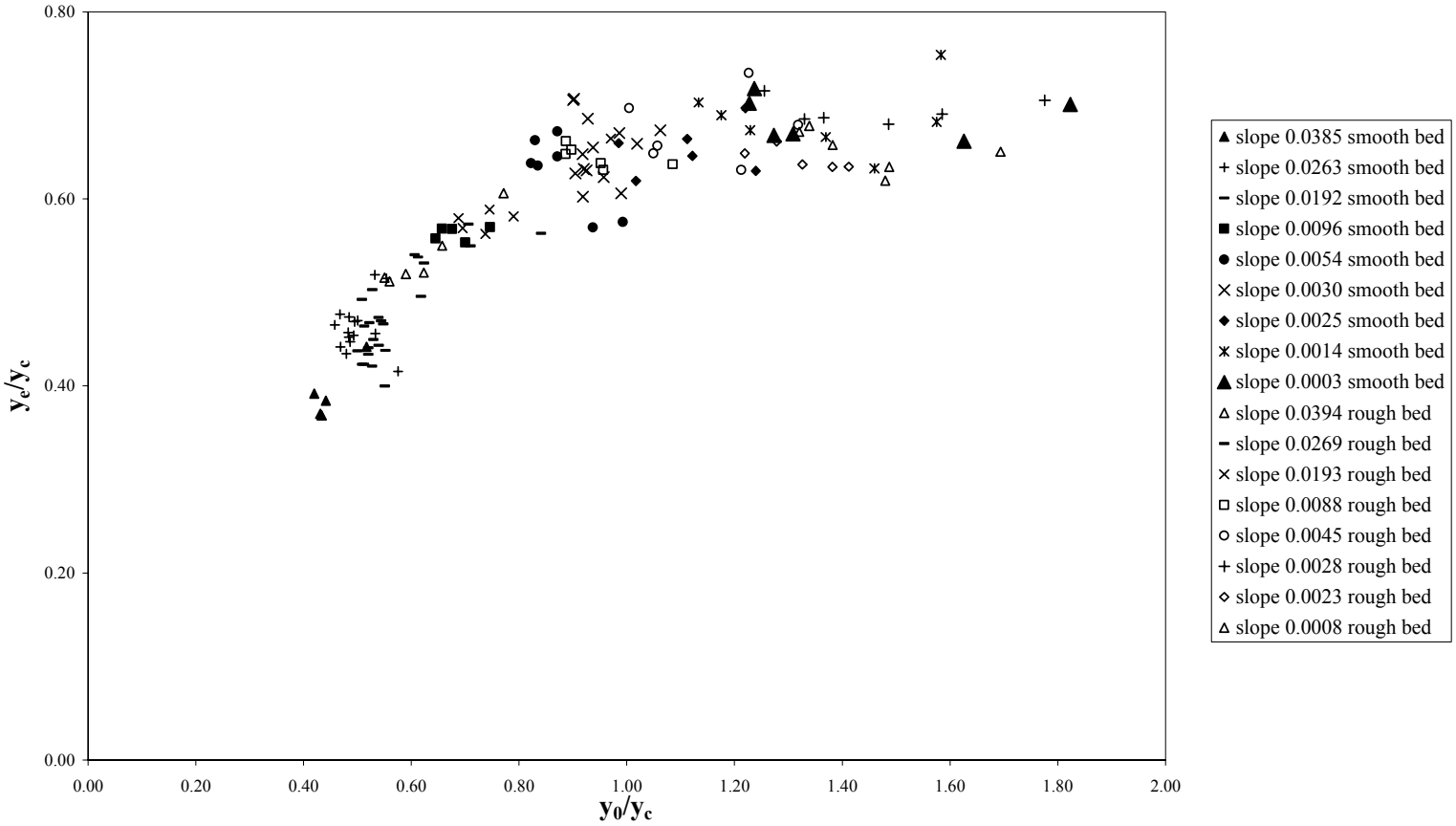

Figure 4.8 Variation of y_e/y_c with y_0/y_c for Slopes of the Present Study

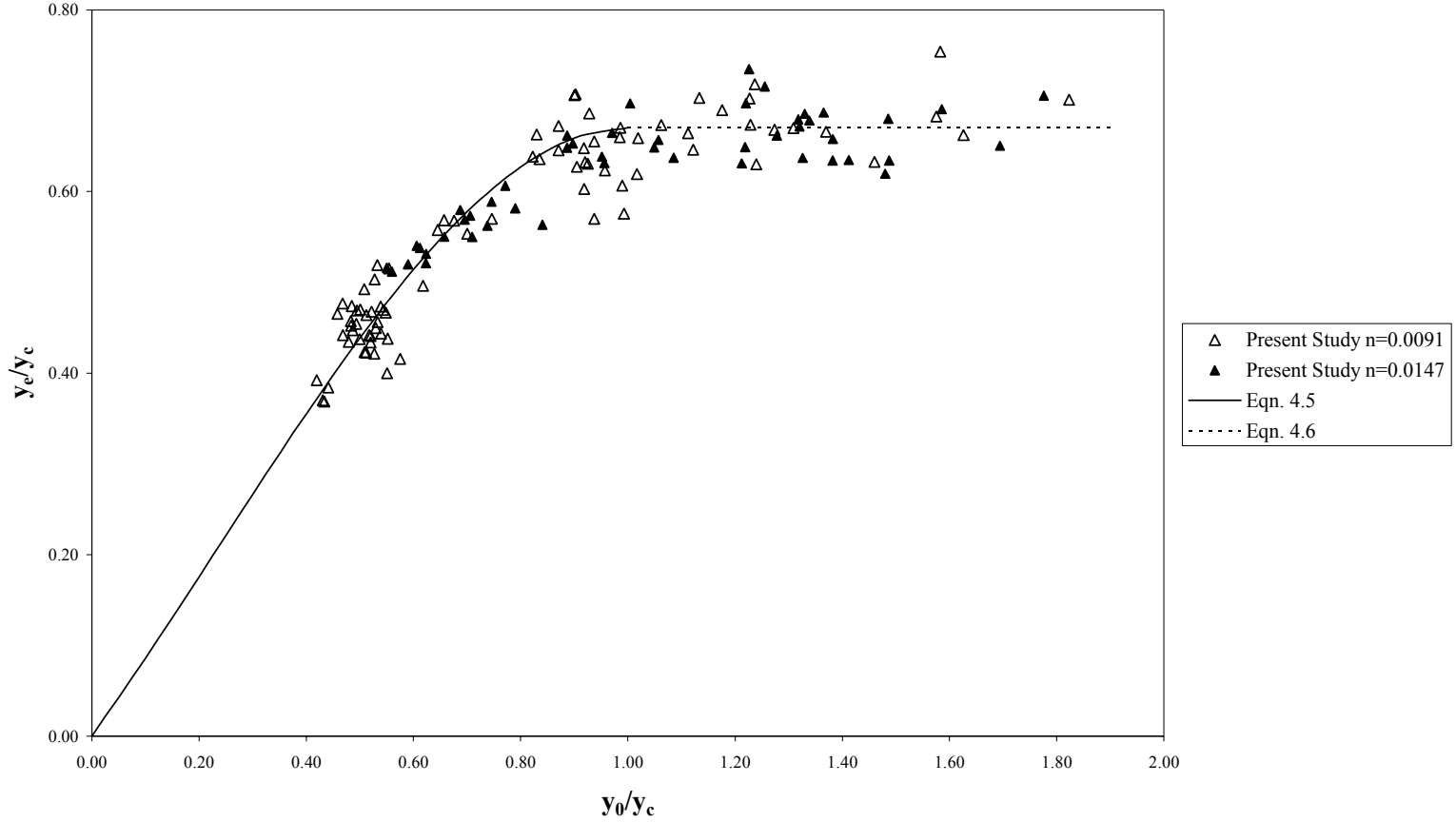

Figure 4.9 Variation of y_e/y_c with y_0/y_c for Smooth and Rough Beds of the Present Study

4.9 Discharge Prediction

The flow rate can be predicted by using the appropriate forms of equations presented above for two combinations of known input parameters, namely $y_e/y_c = f(\sqrt{S_0}/n)$ and $y_e/y_c = f(y_0/y_c)$. The former relation that is given in Equation 4.4 can be rewritten by replacing y_c by $q^{2/3}/g^{1/3}$ as:

$$\frac{y_e}{\sqrt[3]{q^2}} = 1.63 - 0.04\frac{\sqrt{S_0}}{n} \qquad (4\text{-}7)$$

The data and the best fit line whose root mean square, $r^2 = 0.9654$, are depicted in Figure 4.10. In this form, for known channel characteristics (i.e. S_0 and n) for the determination of unit discharge q, the measurement of brink depth is sufficient.

It should be noted that the coefficients in Equation 4.7 are the rounded values. The original values are given in Appendix-A. From Equation 4.7 a design formula for discharge measurement with known brink depth y_e, Manning's roughness coefficient n, and channel bed slope S_0 is obtained. Equation 4.7 can be rearranged as

$$q = \left(\frac{n}{1.63n - 0.04\sqrt{S_0}}\right)^{3/2} y_e^{3/2} \qquad (4\text{-}8)$$

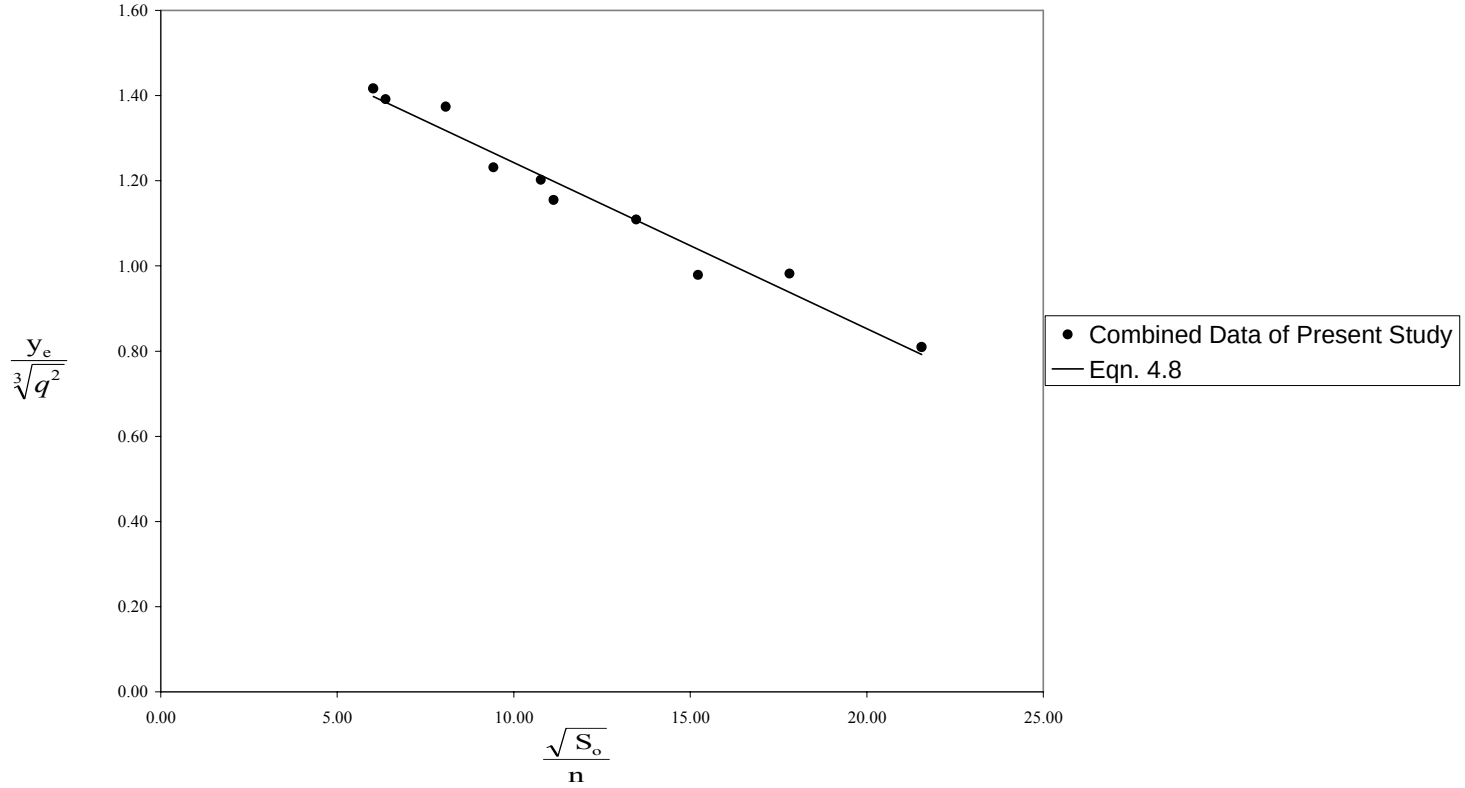

Figure 4.10 Variation of $\frac{y_e}{\sqrt[3]{q^2}}$ with $\frac{\sqrt{S_0}}{n}$ for the Combined Data of the Present Study

The validity of Equation 4.8 is checked by using Alastair et al.'s (1998) data and Turan's (2002) data as a control data. The Equation 4.8 is used to calculate the discharges based on the y_e, S_0 and n values as reported by the authors. The determined values are compared with the respective discharge values reported by them. The best-fit lines are illustrated with $\mp 5\%$ and $\mp 10\%$ confidence interval to confirm Equation 4.8 with the control data collected by other researchers. The correlation coefficient is 0.9859 between the predicted and reported values.

As the correlation turns out to be good; it can be deduced that the Equation 4.8 derived from the present experimental study, is valid.

Equation 4.8 can be used as a very practical discharge measurement device in field studies by Hydraulic engineers due to the fact that there is only brink depth to be measured since slope and roughness of the channel are fixed or determined before. This equation can be presented as an alternative and more practical measurement device to the parshal flume, which is designed to exterminate the sediment problem occurring behind the weirs. In addition, since it is very hard to design and operate the parshal flume, it is very advantageous to use this device in which no other special design is needed. Further, if the brink depth is needed for a design of fall Equation 4.7 can be used for a given discharge, slope and Manning's n.

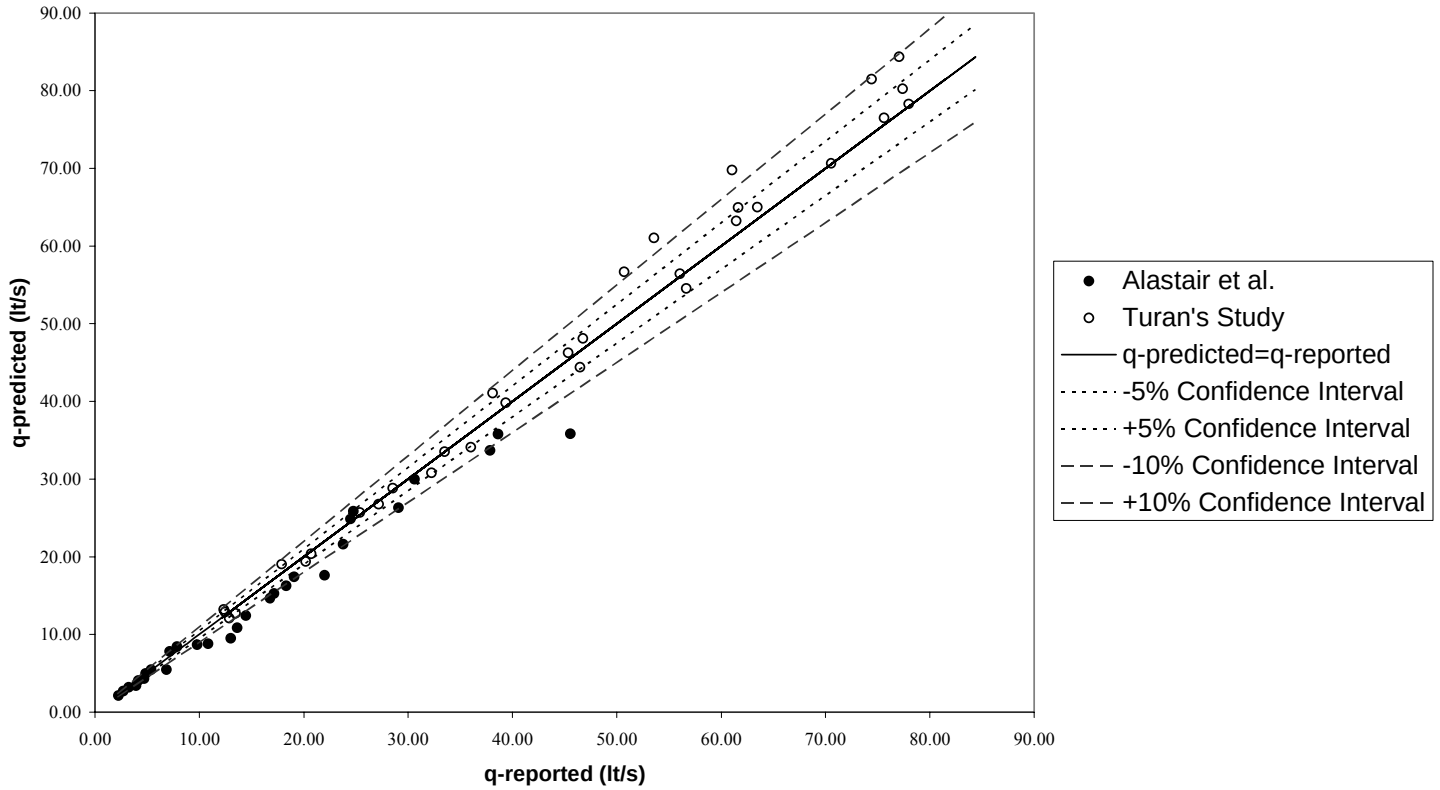

Figure 4.11 Comparing Measured q with Predicted q by Equation 4.8

Since it is quite difficult to identify the exact location of $y_{c,theoretical}$, particularly when q is not known, it is customary to assume the brink depth as the $y_{c,theoretical}$. Yet, the invalidity of this assumption, that is $y_{c,theoretical}$ is nearly equal to y_e, has been proven in this study. In any event, the discharge to be determined using this invalid assumption such that:

$$q_{theoretical} = (g)^{1/2} y_e^{3/2} \qquad (4\text{-}9)$$

is compared with the true value of discharge. The ratio of q_{true} as predicted by Equation 4.8 and $q_{theoretical}$ as determined by Equation 4.9 is obtained as follows:

$$\frac{q_{true}}{q_{theoretical}} = \frac{\left(\frac{n}{1.63n - 0.04\sqrt{S_0}}\right)^{3/2}}{(g)^{1/2}} \qquad (4\text{-}10)$$

The discharge ratios are calculated for several slopes and roughness coefficients as given in Table 4.4. As shown in Table 4.4, the error may be of substantial magnitude.

Table 4.4 Comparison of Discharge Calculation Resulted from the Present Study and Traditional One

S_0	n	$\frac{q_{true}}{q_{theoretical}}$ (%)
0.0385	0.0091	45
0.0003	0.0091	16
0.0394	0.0147	27
0.0088	0.0147	16

CHAPTER 5

CONCLUSIONS and RECOMMENDATIONS FOR FURTHER STUDIES

In the present study the effects of roughness n, slope S_0, Froude number F_0 and normal depth y_0, on the rectangular free overfall at large and on the brink depth y_e, in particular are investigated. An empirical relationship is obtained to estimate discharges. Thus the channel discharges are predicted and are compared with measured values. By this experimental study the following have been discerned:

1. The ratio between the brink depth and theoretical critical depth y_e/y_c, increases as the channel bed slope S_0 decreases, in both subcritical and supercritical flows.

2. For a given bed slope S_0, y_e/y_c ratio increases as the roughness n, increases.

3. Influence of roughness on y_e/y_c, increases with the slope.

4. The brink depth ratio seems to be independent of upstream Froude number for subcritical flows, while it decreases with increasing upstream Froude number for supercritical flows, for both smooth and rough bottoms. In other words, the relation between y_e/y_c and y_0/y_c shows different characteristic

in subcritical and supercritical flow. It is constant for subcritical flow and polynomial for supercritical flow.

5. The end depth ratio for horizontal rectangular channels with critical flow conditions at the upstream can be taken as 0.67.

And, most importantly,

6. Based on the findings of this study an equation of the form in SI system:

$$q = \left(\frac{n}{1.63n - 0.04\sqrt{S_0}}\right)^{3/2} y_e^{3/2} \qquad (4\text{-}8)$$

has been obtained for the determination of discharge in a rectangular and/or wide channel ending in a free overfall. The validity of the above equation has been secured by the use of findings of independently obtained data of the previous works of Alastair et al. (1998) and Turan (2002). In this form, with the known characteristics S_0 and n, for the determination of discharge q, the measurement of the brink depth, y_e, is sufficient. The equation is obtained in the slope range of 0.0003 to 0.0394. This equation can be easily used in the secondary channels of the irrigation system which are made of concrete and have free fall structures.

The followings are recommended for further studies:

1. The effect of bottom roughness and of depth-width ratio must be investigated in more detail in order to extend the range of validity of the discharge equation.

2. Furthermore, the dependence of bottom roughness on Re and depth-width ratio should also be scrutinized to make the discharge equation more robust.

REFERENCES

Alastair, C.D., et al., “Flow measurements in sloping channels with rectangular free overfall”, J. Hydraulic Engng., ASCE, 1998, Vol. 124, No. 7, July

Ali, K. H. M. and Sykes, A., “Free vortex theory applied to free overfall”, J. Hydraulic Div. ASCE, 1972, Vol. 98, May

Bauer, S.W. and Graff, W.H., “Free overfall as flow measurement device”, J. Irrigation and Drainage Div., ASCE, 1971, Vol. 97, No. 1

Chow, V.T., “Open-Channel Hydraulics”, The McGraw-Hill Book Company, New York, Kogakusha Company Limited, Tokyo, 1959.

Delleur et al., “Influence of the slope and roughness on the free overfall”, J. Hydraulic Div. ASCE, 1956, Vol. 82, Aug.

Ferro, V., “Flow measurement with rectangular free overfall”, J. Irrigation and Drainage Div., ASCE, 1992, Vol. 118, No. 6

Ferro, V., “Theoretical end-depth-discharge relationship for free overfall”, J. Irrigation and Drainage Div., ASCE, 1999, Vol. 125, No. 1

Gupta, R.D., et al., “Discharge prediction in smooth trapezoidal free overfall-(positive, zero and negative slopes)”, J. Irrigation and Drainage Div., ASCE, 1993, Vol. 119, No. 2

Gürsoy, E., “Water jet pumps with multiple nozzles”, M.Sc. Thesis METU, Ankara, November 2002.

Hager, W., “Hydraulics of plane free overfall”, J. Hydraulic Engng., ASCE, 1983, Vol. 109, No. 12, Dec.

Henderson, F.M., “Open-Channel Flow”, The Macmillan Company, New York, Collier-Macmillan Limited, London, 1966.

Keller, R.J. and Fong S.S., “Flow measurement with trapezoidal free overfall”, J. Irrigation and Drainage Div., ASCE, 1989, Vol. 115, No. 1

Kökpınar, M.A., Özaydın, V. and Tiğrek, Ş., “Estimation of Manning Roughness Coefficient in a Smooth Rectangular Channel”, Advances in Civil Engineering, IV. International Congress, Eastern Mediterranean University, Gazimagusa, North Cyprus, 2000.

Kraijenhoff, D.A. and Dommerholt, A., “Brink depth method in rectangular channel”, J. Irrigation and Drainage Div., ASCE, 1977, Vol. 103, June

Marchi, E., “On the free overfall”, J. Hydraulic Research, 1993, Vol. 31, No 6

Meadows, M. E. and Walski, T. M. ”Computer applications in Hydraulic Engineering”, Haestad Methods, Inc., 1998

Özsaraç, D., “Potential flow solution for the free overfall”, M.Sc. Thesis METU, Ankara, November 2001.

Rajaratnam, N. And Muralidhar, D., “Characteristics of the rectangular free overfall”, J. Hydraulic Research, 1968, Vol. 6 No. 3

Rajaratnam, N. And Muralidhar, D., “End depth for circular channels”, J. Irrigation and Drainage Div., ASCE, 1964a, Vol. 90, No. 2

Rajaratnam, N. And Muralidhar, D., “End depth for exponential channels”, J. Irrigation and Drainage Div., ASCE, 1964b, Vol. 90, No. 1

Rajaratnam, N. And Muralidhar, D., “Roughness effects on rectangular free overfall”, J. Hydraulic Div. ASCE, 1976, Vol. 102 No. 5

Rouse, H., “Discharge characteristics of the free overfall”, Civil Engineering, 1936, Vol. 6, No. 4

Turan, Ç.K., “Flow measurements in sloping rectangular channels with free overfall”, M.Sc. Thesis METU, Ankara, December 2002.

APPENDIX -A

DATA FOR THE PRESENT STUDY AND THE ORIGINAL FORM OF THE EQUATIONS

Table A.1 The Data For Smooth and Rough Channel.

Experiment No	Channel Slope S_o	Manning's Roughness n	Head on the Triangular Weir. H_w (cm)	Discharge Q(lt/s)	Brink Depth y_e (cm)	Upstream Water Depth y_0 (cm)
1	0.0028	0.0147	52.34	37.53	3.59	6.96
2	0.0028	0.0147	47.67	24.50	2.71	5.38
3	0.0028	0.0147	31.24	1.70	0.47	1.18
4	0.0028	0.0147	59.86	65.85	5.45	9.56
5	0.0028	0.0147	40.76	10.95	1.57	3.42
6	0.0028	0.0147	36.64	5.76	1.04	2.38
7	0.0045	0.0147	38.59	7.98	1.37	2.29
8	0.0045	0.0147	59.76	65.43	5.29	7.62
9	0.0045	0.0147	32.89	2.64	0.61	1.18
10	0.0045	0.0147	51.87	36.08	3.35	5.39
11	0.0045	0.0147	38.65	8.04	1.18	2.27
12	0.0045	0.0147	45.98	20.60	2.28	3.68
13	0.0193	0.0147	44.46	17.40	1.85	2.34
14	0.0193	0.0147	59.38	63.76	4.32	5.13
15	0.0193	0.0147	32.85	2.62	0.59	0.86
16	0.0193	0.0147	53.62	41.68	3.19	3.91
17	0.0193	0.0147	42.11	13.11	1.51	2.05
18	0.0193	0.0147	48.98	27.84	2.41	3.17

Table A.1 The Data For Smooth and Rough Channel, continued.

Experiment No	Channel Slope S_o	Manning's Roughness n	4Head on the Triangular Weir. H_w (cm)	Discharge Q(lt/s)	Brink Depth y_e (cm)	Upstream Water Depth y_0 (cm)
19	0.0394	0.0147	45.93	20.47	1.82	2.06
20	0.0394	0.0147	33.72	3.21	0.62	0.78
21	0.0394	0.0147	39.13	8.66	1.08	1.30
22	0.0394	0.0147	59.71	65.19	3.90	4.16
23	0.0394	0.0147	48.70	27.10	2.16	2.36
24	0.0394	0.0147	39.08	8.60	1.02	1.22
25	0.0088	0.0147	54.70	45.42	3.88	5.33
26	0.0088	0.0147	40.50	10.57	1.42	2.15
27	0.0088	0.0147	56.23	51.01	4.16	5.69
28	0.0088	0.0147	33.26	2.89	0.60	1.03
29	0.0088	0.0147	48.18	25.78	2.70	3.61
30	0.0088	0.0147	41.73	12.47	1.60	2.39
31	0.0023	0.0147	46.81	22.46	2.46	4.75
32	0.0023	0.0147	35.37	4.55	0.81	1.81
33	0.0023	0.0147	37.43	6.61	1.04	2.27
34	0.0023	0.0147	60.22	67.46	5.40	9.45
35	0.0023	0.0147	41.34	11.85	1.55	3.22
36	0.0023	0.0147	51.09	33.73	3.16	5.94
37	0.0008	0.0147	44.23	16.96	1.91	4.56
38	0.0008	0.0147	35.61	4.76	0.86	2.24
39	0.0008	0.0147	59.08	62.48	4.94	9.71
40	0.0008	0.0147	44.37	17.24	1.98	4.64
41	0.0008	0.0147	55.07	46.73	4.11	8.11
42	0.0008	0.0147	50.41	31.75	3.08	6.47
43	0.0269	0.0147	40.21	10.14	1.20	1.55
44	0.0269	0.0147	60.50	68.72	4.23	4.75
45	0.0269	0.0147	32.61	2.46	0.48	0.72
46	0.0269	0.0147	50.58	32.23	2.51	2.95
47	0.0269	0.0147	38.81	8.25	1.09	1.35
48	0.0269	0.0147	48.54	26.69	2.24	2.55
49	0.0385	0.0091	41.40	11.95	0.96	1.02
50	0.0385	0.0091	49.14	28.24	1.60	1.88
51	0.0385	0.0091	58.72	60.94	2.68	3.12
52	0.0385	0.0091	34.88	4.12	0.53	0.62

Table A.1 The Data For Smooth and Rough Channel, continued.

Experiment No	Channel Slope S_o	Manning's Roughness n	4Head on the Triangular Weir. H_w (cm)	Discharge Q(lt/s)	Brink Depth y_e (cm)	Upstream Water Depth y_0 (cm)
53	0.0385	0.0091	62.60	78.60	3.29	3.78
54	0.0263	0.0091	51.22	34.10	2.17	2.30
55	0.0263	0.0091	43.43	15.44	1.38	1.35
56	0.0263	0.0091	51.83	35.94	2.31	2.51
57	0.0263	0.0091	47.74	24.68	1.79	1.92
58	0.0263	0.0091	48.07	25.50	1.85	1.95
59	0.0263	0.0091	35.66	4.81	0.69	0.71
60	0.0263	0.0091	47.06	23.05	1.76	1.73
61	0.0263	0.0091	40.75	10.94	1.05	1.23
62	0.0263	0.0091	53.50	41.29	2.50	2.71
63	0.0263	0.0091	57.57	56.20	3.22	3.43
64	0.0263	0.0091	56.49	51.97	3.05	3.22
65	0.0263	0.0091	48.09	25.55	1.76	1.94
66	0.0263	0.0091	34.45	3.77	0.47	0.65
67	0.0263	0.0091	42.86	14.40	1.31	1.34
68	0.0263	0.0091	35.83	4.96	0.70	0.75
69	0.0192	0.0091	49.39	28.91	2.17	2.24
70	0.0192	0.0091	44.78	18.05	1.62	1.70
71	0.0192	0.0091	44.81	18.12	1.36	1.70
72	0.0192	0.0091	55.52	48.34	2.79	3.28
73	0.0192	0.0091	58.41	59.63	3.35	3.88
74	0.0192	0.0091	56.07	50.39	2.96	3.27
75	0.0192	0.0091	49.95	30.44	1.93	2.32
76	0.0192	0.0091	42.93	14.53	1.22	1.39
77	0.0192	0.0091	36.76	5.88	0.67	0.84
78	0.0192	0.0091	51.27	34.25	2.14	2.56
79	0.0192	0.0091	47.58	24.28	1.66	2.00
80	0.0192	0.0091	37.69	6.90	0.68	0.93
81	0.0192	0.0091	40.49	10.56	1.00	1.21
82	0.0192	0.0091	49.17	28.32	1.91	2.26
83	0.0192	0.0091	57.06	54.21	3.17	3.61
84	0.0192	0.0091	36.33	5.44	0.72	0.89
85	0.0192	0.0091	54.07	43.23	2.69	3.00
86	0.0192	0.0091	41.25	11.71	1.12	1.32
87	0.0096	0.0091	50.02	30.66	2.60	3.01
88	0.0096	0.0091	63.70	84.12	5.00	5.78

Table A.1 The Data For Smooth and Rough Channel, continued.

Experiment No	Channel Slope S_o	Manning's Roughness n	4Head on the Triangular Weir. H_w (cm)	Discharge Q(lt/s)	Brink Depth y_e (cm)	Upstream Water Depth y_0 (cm)
89	0.0096	0.0091	41.89	12.74	1.41	1.78
90	0.0096	0.0091	54.90	46.10	3.41	4.06
91	0.0096	0.0091	36.59	5.71	0.85	1.11
92	0.0054	0.0091	52.47	37.94	3.35	4.40
93	0.0054	0.0091	31.24	1.70	0.38	0.66
94	0.0054	0.0091	60.13	67.05	4.92	6.34
95	0.0054	0.0091	47.66	24.48	2.61	3.27
96	0.0054	0.0091	41.96	12.86	1.72	2.23
97	0.0054	0.0091	40.95	11.25	1.51	2.04
98	0.0054	0.0091	35.68	4.83	0.76	1.25
99	0.0030	0.0091	41.34	11.85	1.60	2.47
100	0.0030	0.0091	45.80	20.20	2.10	3.43
101	0.0030	0.0091	54.16	43.52	4.08	5.20
102	0.0030	0.0091	55.70	49.01	4.29	5.81
103	0.0030	0.0091	47.72	24.63	2.59	3.71
104	0.0030	0.0091	38.55	7.92	1.25	1.97
105	0.0030	0.0091	50.83	32.96	3.11	4.41
106	0.0030	0.0091	46.19	21.06	2.22	3.41
107	0.0030	0.0091	49.90	30.31	2.87	4.18
108	0.0030	0.0091	46.87	22.60	2.25	3.43
109	0.0030	0.0091	45.12	18.75	2.21	3.25
110	0.0030	0.0091	50.71	32.61	2.99	4.31
111	0.0030	0.0091	57.28	55.06	4.78	6.10
112	0.0030	0.0091	51.46	34.82	3.14	4.61
113	0.0025	0.0091	46.98	22.87	2.33	3.83
114	0.0025	0.0091	39.44	9.08	1.35	2.26
115	0.0025	0.0091	39.34	8.94	1.30	2.26
116	0.0025	0.0091	33.33	2.94	0.60	1.19
117	0.0025	0.0091	57.33	55.24	4.47	6.67
118	0.0014	0.0091	49.89	30.29	3.13	5.34
119	0.0014	0.0091	36.02	5.14	0.93	1.91
120	0.0014	0.0091	59.11	62.58	5.18	8.34
121	0.0014	0.0091	31.04	1.61	0.48	1.01
122	0.0014	0.0091	43.56	15.67	1.97	3.59
123	0.0014	0.0091	31.92	2.06	0.52	1.19
124	0.0014	0.0091	33.05	2.75	0.58	1.34

Table A.1 The Data For Smooth and Rough Channel, continued.

Experiment No	Channel Slope S_o	Manning's Roughness n	4Head on the Triangular Weir. H_w (cm)	Discharge Q(lt/s)	Brink Depth y_e (cm)	Upstream Water Depth y_0 (cm)
125	0.0003	0.0091	45.07	18.65	2.20	4.30
126	0.0003	0.0091	31.78	1.98	0.52	1.34
127	0.0003	0.0091	59.41	63.90	5.24	9.16
128	0.0003	0.0091	55.66	48.87	4.48	7.72
129	0.0003	0.0091	48.73	27.18	2.82	5.38
130	0.0003	0.0091	35.30	4.48	0.84	2.06

Note: For Table A.1 the upstream water depth, y_0 , values are measured at predetermined intervals. The values presented here are the average of the measured upstream water depth values.

Table A.2 The Original Form of the Equations

Equation No.	Equation	r^2
4.2	$\frac{y_e}{y_c} = 0.7786 - 2.0497\sqrt{S_0}$	0.9708
4.3	$\frac{y_e}{y_c} = 0.7625 - 1.2882\sqrt{S_0}$	0.9604
4.4	$\frac{y_e}{y_c} = 0.7626 - 0.0182\frac{\sqrt{S_0}}{n}$	0.9654
4.5	$\frac{y_e}{y_c} = -0.5133\left(\frac{y_0}{y_c}\right)^3 - 0.3565\left(\frac{y_0}{y_c}\right)^2 + 0.8269\left(\frac{y_0}{y_c}\right)$	0.9526
4.6	$\frac{y_e}{y_c} = 0.6701\left(\frac{y_0}{y_c}\right)$	0.9526
4.7	$\frac{y_e}{\sqrt[3]{q^2}} = 1.6326 - 0.039\frac{\sqrt{S_0}}{n}$	0.9654
4.8	$q = \left(\frac{n}{1.6326n - 0.039\sqrt{S_0}}\right)^{3/2} y_e^{3/2}$	0.9654

APPENDIX -B

VARIATION OF UPSTREAM WATER DEPTH

In order to ensure the safeness of the procedure followed throughout the study, data collected are checked by calculations using relevant equations. The comparison between the measured normal depths with the calculated normal depths using Manning's equation is performed to verify the logic and security of the study. In Figure A.1 the variation of measured normal depth, y_0 and predicted normal depth is given for smooth channel. In the same manner in Figure A.2, the same variation is given for rough channel. The results were in good agreement except the values of the mildest slopes 0.0003 for smooth channel and 0.0008 for rough channel. In the mildest slopes the calculated y_0 were incoherent with the measured y_0 because the Manning equation loses its validity at horizontal or nearly horizontal slopes like in this case, which was an expected result. Therefore in Figures A.1 and A.2 the mildest or nearly horizontal slopes were excluded. In Figure A.1, the following equation for smooth channel is obtained:

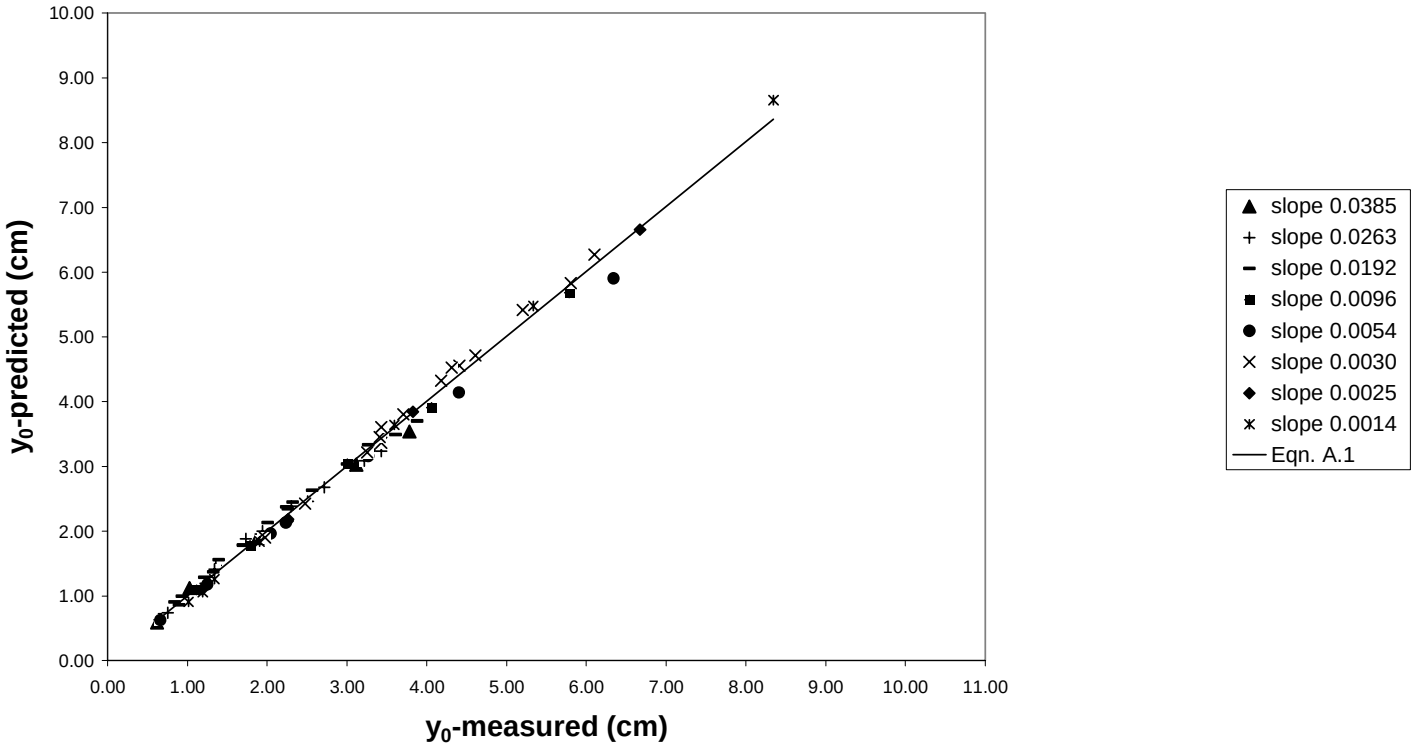

Figure A.1 Comparing Measured y_0 with Predicted y_0 by Manning's Equation for Smooth Channel

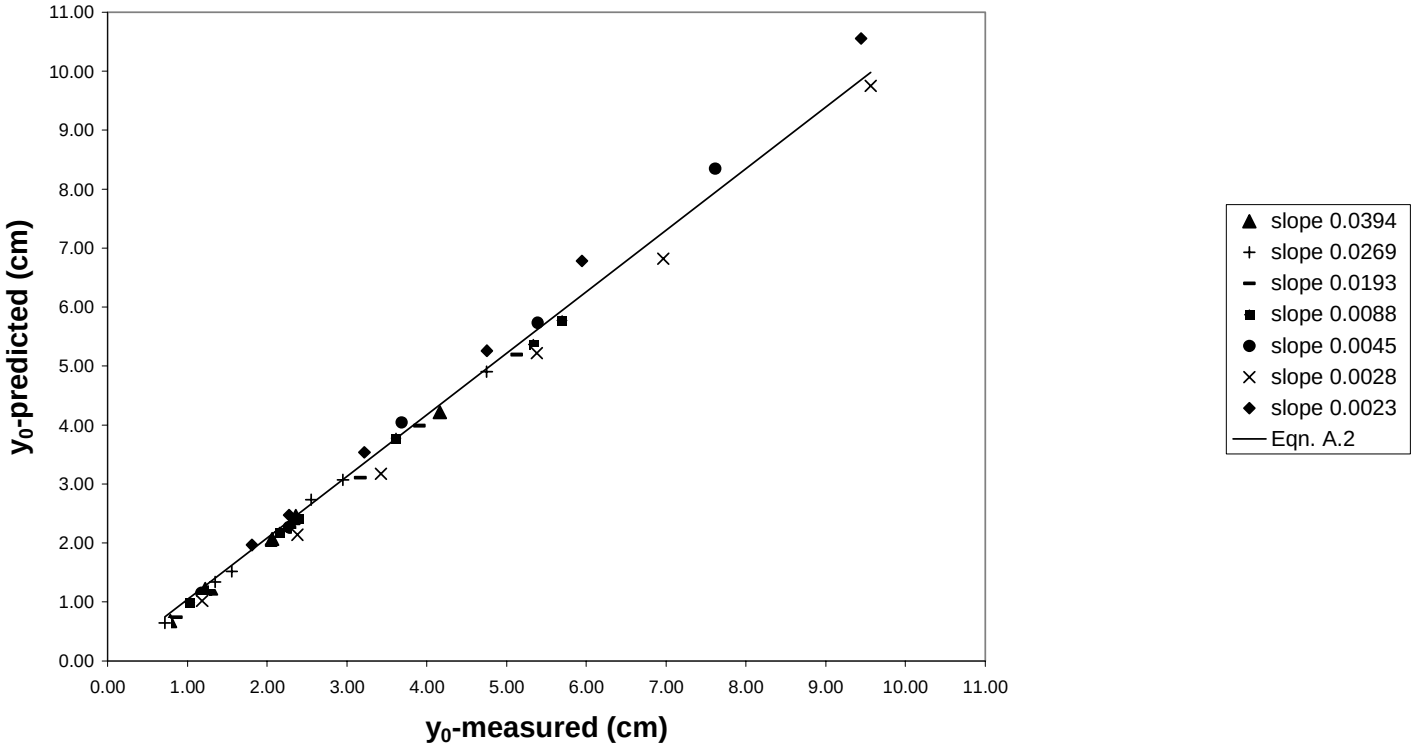

Figure A.2 Comparing Measured y_0 with Predicted y_0 by Manning's Equation for Rough Channel

$$y_{0\,predicted} = 1.002\, y_{0\,measured} \qquad (A.1)$$

The root mean square, $r^2 = 0.9945$

The same linear relationship for rough channel inferred from Figure A.2 is:

$$y_{0\,predicted} = 1.0433\, y_{0\,measured} \qquad (A.2)$$

The root mean square, $r^2 = 0.9906$

From above equations, it can be deduced that the measured normal depths are in reasonable agreement with the predicted normal depths with considerably sensible root mean square values.

It should be noted that the particular study, explained here above, is performed to achieve a good predictor of the location of the normal depth.